

# 1 **Sediment Quality Assessment in an industrialized Greek coastal 2 marine area (West Saronikos Gulf)**

3 Georgia Filippi, Manos Dassenakis, Vasiliki Paraskevopoulou, Konstantinos Lazogiannis

4 Laboratory of Environmental Chemistry Department of Chemistry, National and Kapodistrian University of Athens, Athens,  
5 15784, Greece

6  
7 *Correspondence to:* Georgia Filippi (mphilippi@chem.uoa.gr)

9 **Abstract.** Eight sediment cores from the coastal marine area of West Saronikos Gulf have been analyzed for grain size and  
10 geochemistry. The concentrations of eight metals (Al, Fe, Mn, Cu, Cr, Ni, Pb and Zn) along with total organic carbon (TOC)  
11 and carbonate content were measured. The cores are fairly homogeneous, in terms of carbonates and the down-core variability  
12 of % TOC, is characterized by high surficial values that decrease with depth. Metal concentrations from both geological (Al,  
13 Mn, Cr, Ni) and anthropogenic origin (Cu, Pb, Zn), are higher in the muddy than the sand fraction of sediments. The spatial  
14 distribution of Al, Fe, Mn, Cu, Pb and Zn in surface sediments presents increasing concentrations from the northeast to the  
15 southwest part of the study area, from the shallow to the deeper parts in contrast to Cr and Ni which are increased in the  
16 northern nearshore stations. Based on the vertical distributions, the metal to Al ratios of Cu, Pb and Zn show a constant decrease  
17 over depth along most cores, indicating the anthropogenic effects to surface sediments, while Fe/Al is constant. Spearman's  
18 correlation analysis performed among the fine grain metal contents, demonstrated a strong positive correlation ( $r > 0.5$ ,  $p <$   
19 0.05) between Al, Fe, Mn, Cu, Pb and Zn. The calculated enrichment factors indicate minimal to moderate pollution. The  
20 concentrations of Cr at most surface sediments are higher than the ERL value ( $81 \text{ mg Kg}^{-1}$ ) but below the ERM value ( $370 \text{ mg}$   
21  $\text{Kg}^{-1}$ ) and the concentrations of Ni are always higher than the ERM value ( $51.6 \text{ mg Kg}^{-1}$ ). In contrast, the concentrations of  
22 Cu, Pb, Zn, at most surface sediments, are below ERL values. The mean effects range medium quotients (mERMq) of surface  
23 sediments, based on the overall metal concentrations indicated that the surface sediments of most cores, are moderately toxic.  
24 The levels of Cr, Ni, Mn and Zn at most stations are decreased in 2017, but the concentrations of Pb and Cu are increased in  
25 2017, compared to a previous study of 2007. The concentrations of Cu, Pb and Zn in the surface sediments of West Saronikos  
26 Gulf are lower than levels reported for Inner Saronikos Gulf, Elefsis Bay and other polluted hot spot areas of Greece, owing  
27 to a lower degree of urban and industrial development.

28  
29 **Copyright statement:** The copyright statement will be included by Copernicus, if applicable.

## 30 **1 Introduction**

31 Sediment cores are one of the most easily accessed natural archives, used to evaluate and reconstruct historical pollution trends  
32 in aquatic environments. The cores provide data to characterize sediment physical properties and their geochemistry and  
33 composition. Vertical profiles of heavy metals can present sedimentation rate, changes in diagenetic processes and evolution  
34 of human pressures. Metals released into aquatic systems, undergo several processes, such as adsorption, photolysis, chemical  
35 oxidation and microbial degradation. Sedimentation depends on the contaminant physicochemical properties, the sediment  
36 physical properties, the adsorption capabilities and the partitioning constant at the water-sediment interface. Trace metals  
37 removed from the water column are adsorbed on particulate matter and eventually deposited on bottom sediments (Bigus et  
38 al. 2014).

39 Sediments are repositories for metals such as chromium, lead, copper, nickel, zinc and manganese that present as discrete  
40 compounds, ions held by cation-exchanging clays, bound to hydrated oxides of iron and manganese, or chelated by insoluble

41 humic substances. Solubilization of metals from sedimentary or suspended matter depends on the presence of complexing  
42 agents. Metals that are held by suspended particles and sediments are less available than those in true solution (Manahan,  
43 2011).

44 Saronikos Gulf (Greece) is a marine area of the Aegean Sea between the peninsulas of Attiki and Argolida. The environmental  
45 interest in Saronikos gulf arises from the fact that it is the marine border of the most urbanized areas of Greece, i.e., the  
46 country's capital (Athens), the industrial zones of Attiki (Elefsis, Thriasio, Sousaki) and the large port city of Piraeus. As a  
47 result, there have been on going environmental monitoring and oceanographic studies of Saronikos since the 80's. There are  
48 several published works focusing on the eastern part of Saronikos due to the presence of extended and intensive anthropogenic  
49 activities (Scoullos, 1986; Pavlidou et al., 2004; Scoullos et al., 2007; Kontogiannis, 2010; Paraskevopoulou et al., 2014;  
50 Pangiotoulias et al., 2017; Karageorgis et al., 2020; Prifti et al., 2022). In contrast, fewer studies have focused on North West  
51 Saronikos despite the presence of a less extensive industrial zone hosting a major oil refinery and coastal touristic activities  
52 along with a particular geological (volcanic/hydrothermal) background (Paraskevopoulou, 2009; Kelepertsis et al., 2001).  
53 The main aim of this work is to assess the levels and the distribution of several heavy metals (Al, Fe, Mn, Pb, Zn, Ni, Cr, Cu)  
54 in sediment cores of West Saronikos, in order to discern between the relative contribution of geological and anthropogenic  
55 origins and to identify the major sources of metal pollution. The second aim is to determine the evolution of marine pollution  
56 in the area by comparing the results with those of a similar study ten years ago, conducted at the Laboratory of Environmental  
57 Chemistry (Department of Chemistry, National and Kapodistrian University of Athens). The last aim of this work is to assess  
58 and highlight the differences between the concentrations of heavy metals in the surface sediments of West Saronikos in  
59 comparison to sediments in studies conducted in East Saronikos, Elefsis bay and other areas of Greece.

## 60 **2 Study area**

61 Saronikos Gulf is situated at the central Aegean Sea (north east Mediterranean) between  $37^{\circ}30'N$ - $38^{\circ}00'N$  and  $24^{\circ}01' E$ -  
62  $23^{\circ}00' E$  formed between the peninsulas of Attiki and Argolida. The length of its coastline is 270 km, the surface is  $2.866 km^2$   
63 and the mean water depth 100 m. To the north, a shallow (30 m depth) embayment is formed, known as Elefsis bay. The  
64 islands of Salamina and Aigina and the plateau between them, divide the gulf into two basins: the western basin (Western  
65 Saronikos Gulf) with maximum depths of 220 m in the north and 440 m in the south and the eastern basin which has a smooth  
66 bathymetry with depths of 50-70 m to the north (Inner Saronikos Gulf) reaching 200 m to the southeast, from where the gulf  
67 opens to the Aegean Sea (Outer Saronikos Gulf). To the west, the narrow Isthmus of Corinth connects Korinthiakos Gulf with  
68 Saronikos Gulf in the Aegean Sea (Kontoyiannis, 2010; Paraskevopoulou, 2014).

69 The gulf is subjected to a strong seasonal cycle of heating and cooling, with air temperatures between 0 - 40 ° C, which causes  
70 the formation of a seasonal pycnocline from May to November. In winter, the water column is homogenized down to 120 m.  
71 However, in the western part, vertical mixing never reached the sea bottom (440 m) in the years after 1992 and dissolved  
72 oxygen concentration has approached nearly anoxic conditions (D.O. < 1mL/L) (Paraskevopoulou et al., 2014).

73 A few circulation studies have been conducted in Saronikos in order to discern the possible movement of the treated wastewater  
74 effluent discharged at 65m south of Psittalia island in the eastern basin. The circulation is reported as strongly dependent on  
75 local winds with predominant northerly direction throughout the year. However, westerly and southerly winds may also occur  
76 in fall, winter and spring. Under the predominant northerly wind regime in summer and fall during the presence of the seasonal  
77 pycnocline there is a distinctly different two-layer circulation above and below 60m. In the upper layer there is a general  
78 eastward anticyclonic (clockwise) flow from the west to the east basin. Below 60m the flow is reversed from the northeast  
79 through the Salamina-Aigina passage to the southwest towards the deeper part of the west basin following a cyclonic  
80 (counterclockwise) path. During winter when the water column is fully mixed down to 90m the general flow is anticyclonic  
81 from the west to east. Nearshore on the northwest Sousaki coast the currents reported are directed from the north to the south.

82 In spring during the pycnocline formation there is no continuous flow structure spanning both the west and east basins. In the  
83 west during spring there is a rather strong north to south flow (SoHelME, 2005; Kontoyiannis, 2010).  
84 Saronikos gulf, as a whole, is subjected to intense anthropogenic pressure, as it is the marine border of the cities of Athens and  
85 Piraeus with 3-4 million inhabitants. Several point and non-point pollution sources are present mainly on the northeastern  
86 coasts. One of the most important point sources is the Athens/Pireaus wastewater treatment plant (WWTP) on the small island  
87 of Psittalia, among the largest in Europe, with a population equivalent (p.e.) coverage of 5.6 million. Other point sources along  
88 the coasts include the port of Piraeus, marinas, touristic facilities, fish farms and the effluents of smaller towns and settlements.  
89 Finally, pollution pressure arises from increased marine traffic, since Piraeus is one of the largest and busiest Mediterranean  
90 ports, and from the heavy vehicle traffic and the heating systems in the extended urban areas (Paraskevopoulou et al., 2014).  
91 The coastal marine area of the north part of West Saronikos Gulf is affected by a few types of industries established there  
92 during the 1970's, that include a major oil refinery unit at the center of Susaki area, a cable manufacturer, soya mills, sulfur /  
93 fertilizers manufacturing for agricultural use and the increased sewage load from nearby coastal villages due to the summer  
94 tourist season (Kelepertsis et al., 2001; Paraskevopoulou, 2009). The settlements on the coast of West Saronikos, to the best  
95 of our knowledge, are not yet connected to wastewater treatment facilities and a projected treatment plant in Aghioi Theodoroi  
96 is under construction. The Susaki area, which extends parallel to the northern coast of West Saronikos for about 8 Km, is  
97 known for its volcanic activity which took place during Pliocene-Quaternary. Most of the volcanic materials were transported  
98 by fluvial processes and deposited in the alluvial plains and coastal regions. The formations observed are peridotites and  
99 serpentinites, neogene deposits and Quaternary deposits. As a result, elevated values of Cr, Ni, Co, Mn, Fe are found in the  
100 soils and sediments of this area and can be explained by the existence of the ultrabasic rocks (Kelepertsis et al., 2001). The  
101 southwest deeper part of West Saronikos (Epidavros basin) could be affected by the transport of organic and inorganic  
102 pollutants from the eastern basin due to the periodical northeast to southwest water flow below the pycnocline (Psyllidou-  
103 Giouranovits and Pavlidou, 1998; Kontoyannis, 2010).

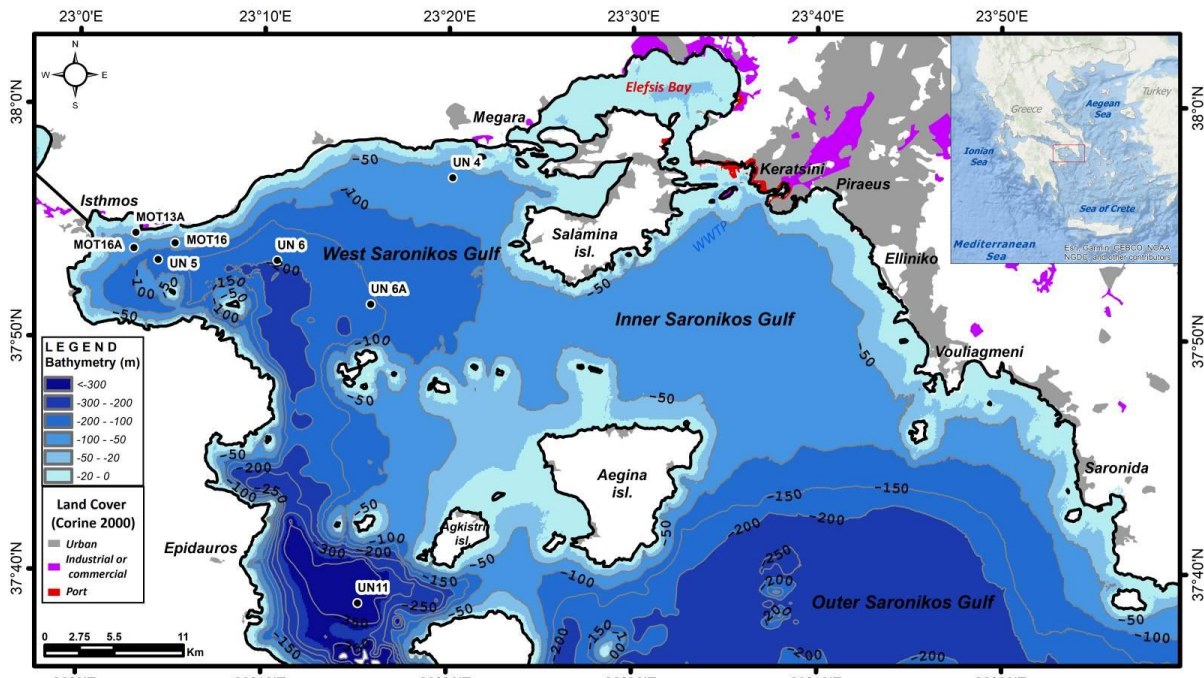
### 104 **3. Materials and methods**

105 Eight short sediment cores (12-32 cm) were obtained at corresponding number of stations with varying depths (50-420 m) in  
106 the area of West Saronikos Gulf with the use of a box corer. The sampling was conducted on 18 October 2017 with the Greek  
107 Oceanographic vessel RV *Aegaeo*. The West Saronikos Gulf study area and the specific location of stations are presented in  
108 Fig. 1.

109  
110 **Table 1. Coordinates, water column depth and core length at each sampling station.**

| Station | Latitude N<br>(dec.minutes) | Longitude E<br>(dec.minutes) | Depth (m) | Core length (cm) |
|---------|-----------------------------|------------------------------|-----------|------------------|
| MOT13A  | 37° 54.602                  | 23° 03.184                   | 50        | 12               |
| MOT16A  | 37° 53.995                  | 23° 03.080                   | 100       | 32               |
| UN5     | 37° 53.459                  | 23° 04.393                   | 140       | 32               |
| MOT16   | 37° 54.179                  | 23° 05. 312                  | 85        | 20               |
| UN6     | 37° 53.455                  | 23° 10. 857                  | 193       | 26               |
| UN6A    | 37° 51.610                  | 23° 15.932                   | 165       | 24               |
| UN4     | 37° 57.057                  | 23° 20.331                   | 79        | 22               |
| UN11    | 37° 38.800                  | 23° 15.338                   | 420       | 32               |

111  
112 Stations MOT13A, MOT16A, UN5, MOT16, UN6 (near the Susaki area) and UN4 (Megara basin), at the north-western part,  
113 are affected by the coastal industrial zone, urbanization and touristic activities. The offshore station UN6A, at the middle of  
114 Megara basin, is probably less disturbed by anthropogenic activities. Finally, station UN11, in Epidavros basin at the southwest  
115 part of the study area, is influenced by trawling and aquaculture and potential transport of organic and inorganic pollutants  
116 from eastern Saronikos due to periodical circulation patterns in the water layers below 60m.  
117



118  
119 **Figure 1: Study area of West Saronikos Gulf and sampling stations (The map was constructed using Arc Map with bathymetry**  
120 **representation data from the European Marine Observation and Data Network-EMODnet: <https://portal.emodnet-bathymetry.eu/>**  
121 **and land cover data from Corine 2000).**

122

123 The cores were frozen immediately after sampling and cut in 1cm layers down to the top 10cm of each core and 2cm layers  
124 after that. The separated layers were stored frozen until further processing. The initial step of analysis is removal of water  
125 content with the use of a Lab Conco freeze-dryer. Subsequently, grain size analysis via dry sieving was performed using the  
126 1mm and 63 $\mu$ m Retsch stainless steel sieves. The gravel (>1mm), sand (>63 $\mu$ m) and muddy (<63 $\mu$ m) fractions were separated  
127 for the calculation of the respective percentages to the total sediment. The gravel fraction was discarded. Total organic carbon,  
128 carbonates and the concentrations of heavy metals were determined separately in both sand and muddy sediment, when the  
129 fraction percentage was more than 10 % of the total sediment or in the prevailing fraction only (above 90%). Table 1 presents  
130 the coordinates and depth of each sampling station along with the corresponding core length.

131 The total organic carbon (TOC) content was measured using the standard Walkley (1947) method as modified by Jackson  
132 (1958) and Loring & Rantala (1992), which is based on the exothermic reaction (oxidation) of the sediment with potassium  
133 dichromate ( $K_2Cr_2O_7$ ) and concentrated sulfuric acid ( $H_2SO_4$ ), followed by back-titration with ferrous ammonium sulfate  
134 ( $FeSO_4$ ) and ferroine indicator.

135 The carbonate content was determined by calculating the weight difference of the sample before and after the strong  
136 effervescence caused by adding hydrogen chloride (HCl) 6 M to the sediment causing an exothermic reaction followed by HCl  
137 gas and  $CO_2$  emission (Loring and Rantala, 1992).

138 The total metal contents were extracted via complete dissolution of sediment samples with an acid mixture of  $HNO_3$ - $HClO_4$ -  
139 HF (ISO-14869-1:2000) (Peña-Icart et al., 2011). Then, the total metal concentrations were determined by Flame or Graphite  
140 Furnace Atomic Absorption Spectroscopy (FAAS-Varien SpectrAA-200 and GFAAS- Varien SpectrAA 640Z) (Skoog et al.,  
141 1998). In order to evaluate the precision and accuracy of the method for total metal analysis a certified reference material  
142 (PACS-3, NRC-CNRC) was carried through the analytical procedure along with the sediment samples in every digestion batch  
143 and 1 or 2 random layers of each core were also analyzed in duplicate. Accuracy was calculated as % recovery (percentage  
144 ratio of the measured to the certified value). The precision was evaluated using the % RSD-Relative Standard Deviation  
145 (percent ratio of the standard deviation to the average concentration of the replicates) calculated for each metal by each of the  
146 duplicate measurements (repeatability estimation) and the multiple measurements of the reference material (reproducibility  
147 estimation). The quality data for the total metal method are presented in the Appendix (Table A1). The precision and recoveries

149 generally fall into the ranges 3-10% RSD and 80-120 % recovery, depending on analyte level. Such results of analytical  
150 performance are anticipated for multistage analysis of solid samples and are roughly recommended by the US Environmental  
151 Protection Agency (US EPA) and the Association of Official Analytical Chemists (AOAC) (US EPA, 1996; AOAC  
152 International, 2016). For every core the %RSD for each metal was calculated as an indication of the downcore variability and  
153 the results are presented in Fig. A1 – A15 (Appendix A).

154 Most statistical treatment of data and the vertical distribution graphs were performed by Microsoft Excel 2010. The horizontal  
155 distributions of metals were visualized with the software package Ocean Data View (ODV) 2017. The software IBM-SPSS  
156 Statistics 2020 was used for statistical comparisons between stations regarding the trace metal concentrations and Spearman  
157 correlation analysis to identify significant relationships between different heavy metals, total organic carbon and carbonates.  
158 The comparison between stations was done by performing parametric (One-Way Anova) and non-parametric (Kruskal Wallis,  
159 Kolmogorov-Smirnov) tests between the mean values and standard deviations calculated for each metal and each core by the  
160 results of the top 5 cm. The comparison between two groups of values, e.g. a variable between two cores or concentrations of  
161 variables above-below a certain layer in a single core was either done by two-sided t-test or by the non-parametric equivalents  
162 Mann-Whitney and Kolmogorov-Smirnov tests. In all comparative tests statistical results were calculated at the 95%  
163 confidence level (p<0.05).

## 164 **4 Results**

### 165 **4.1 Geochemical results**

166 Table 2 summarizes the main findings from the determination of geochemical parameters. The grain size in cores from stations  
167 MOT16A, UN5, UN6, UN6A, UN11, is dominated by mud, while the percentage of sand fraction is generally low and below  
168 10% in most core layers. On the other hand, in cores MOT13A, MOT16, UN4 the percentages of both sand (39-66%) and mud  
169 (15-50%) are significant. The sediments at stations MOT13A and MOT16 are coarser with average mud percentages 25 and  
170 38% respectively, while at station UN4 especially in the top 10cm the average mud percentage is slightly increased (43%). As  
171 a result, the percentages of total organic carbon (TOC) and carbonates as well as the concentrations of heavy metals were  
172 determined in the mud fraction (<63µm) of sediments in cores MOT16A, UN5, UN6, UN6A and UN11 and separately in the  
173 sand and mud fraction of sediments in cores MOT13A, MOT16 and UN4.

174

175 **Table 2. Summary statistics of grain size percentages, TOC and carbonate content along the collected cores.**

| Station | % sand |     | % mud (silt and clay) |     | % TOC |      | % CO <sub>3</sub> <sup>2-</sup> |     |
|---------|--------|-----|-----------------------|-----|-------|------|---------------------------------|-----|
|         | Min    | Max | Min                   | Max | Min   | Max  | Min                             | Max |
| MOT13A  | 51     | 66  | 15                    | 38  | 0.45  | 0.92 | 26                              | 28  |
| MOT16A  | 1      | 23  | 77                    | 99  | 0.10  | 0.93 | 22                              | 23  |
| UN5     | 1      | 14  | 86                    | 99  | 0.44  | 1.12 | 20                              | 23  |
| MOT16   | 47     | 65  | 29                    | 45  | 0.33  | 1.28 | 20                              | 22  |
| UN6     | 1      | 32  | 68                    | 99  | 0.57  | 2.44 | 19                              | 23  |
| UN6A    | 1      | 22  | 78                    | 99  | 0.33  | 1.32 | 22                              | 25  |
| UN4     | 39     | 60  | 20                    | 50  | 0.51  | 0.75 | 29                              | 33  |
| UN11    | 0      | 15  | 74                    | 100 | 0.77  | 2.35 | 15                              | 19  |

176

177 Apart from small variations, the cores are fairly homogeneous, in terms of carbonates. The high percentages of % CO<sub>3</sub><sup>2-</sup> in  
178 cores MOT13A and UN4 are associated with the coarse - grained samples and abundant presence of shell fragments. Figure 2  
179 presents the vertical distribution of % TOC in selected cores. Comparing between stations the lowest TOC values in the top  
180 5cm are measured in the coarser sediments of MOT13A (average 0.57%) and the highest in the deepest station UN11 (average  
181 1.74%). There was no statistical difference between TOC in the remaining cores and the average values for the top 5cm are  
182 the following: UN4 (0.68%), MOT16A (0.69%), MOT16 (0.96%), UN5 (0.96%), UN6A (1.09%) and UN6 (1.26%).

183

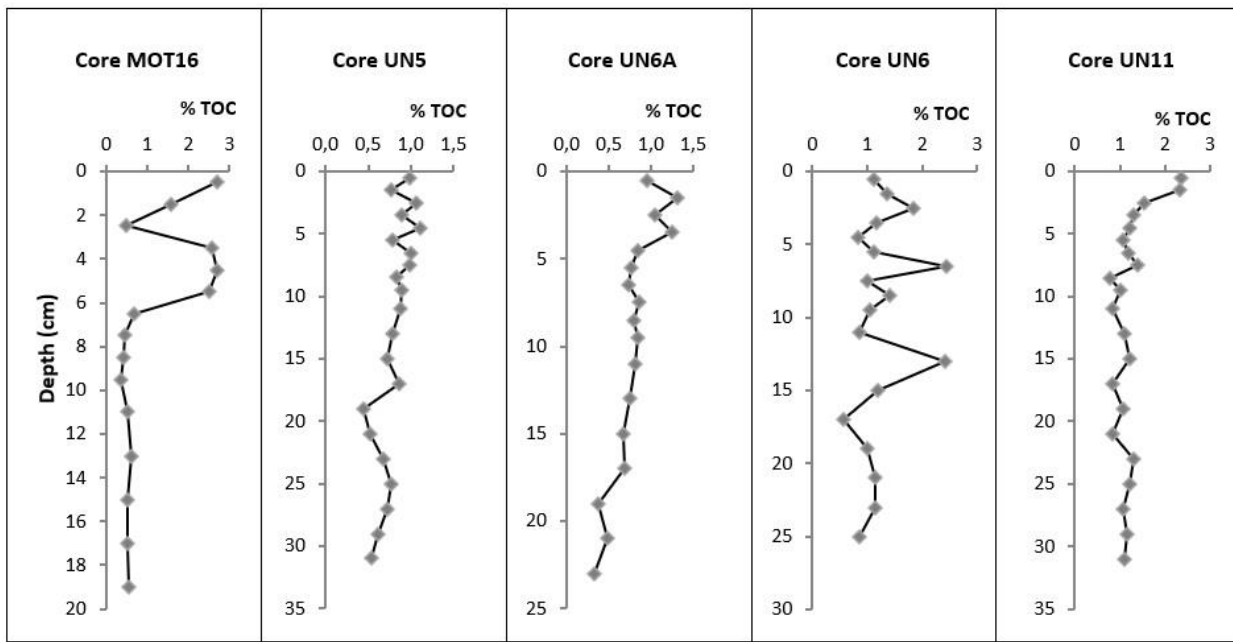


Figure 2: Vertical distribution of % TOC at selected cores [MOT16 profile depicts fine sediment (< 63  $\mu$ m) TOC content].

184

185  
186

187 The vertical TOC distribution in core MOT16 is differentiated than the corresponding in the adjacent station MOT13A. Below  
188 6cm the levels of TOC are similar in both stations. However, in the top 6cm of core MOT16 average TOC in the total sediment  
189 is approximately 1% while below 6cm the corresponding average is 0,42%. This is caused by a striking increase in the TOC  
190 content of the muddy sediments, with an average of 2.4% TOC at the top 6cm approximately 5-fold higher than the  
191 corresponding in the deeper layers (0.5%). At the same time the TOC variability in the sandy fraction of the top 6cm of MOT16  
192 is minimal, ranging between 0.3% and 0.4%. The vertical TOC distributions of the dominantly muddy cores (MOT16A, UN5,  
193 UN6, UN6A, UN11) present high surficial content and gradual increase with depth.

194 Table 3 presents TOC, carbonate and heavy metal contents in the two fractions (sand-mud) at the shallow coarse-grained cores  
195 MOT13A, MOT16, UN4. It is apparent that the % TOC content of the muddy material is higher than the corresponding content  
196 of the sandy fraction as anticipated. The %  $\text{CaCO}_3$  content is increased in the sandy material of cores MOT13A, UN4 compared  
197 to that of the fine sediment and is approximately equal in the two sediment fractions of core MOT16.

198 The concentrations of Al, Cr, Cu, Mn, Pb, Ni and Zn are higher in the muddy sediments of MOT13A and UN4 than the  
199 corresponding values in sandy sediments. The same applies to Al, Mn, Cu, and Zn in MOT16. Unlike other metals the Fe  
200 content is more or less similar in both sediment fractions of cores MOT13A and UN4. The sediments of core MOT16 appear  
201 to be different with higher concentrations of Fe, Cr, Ni and Pb in the coarse-grained fraction.

202 The vertical distributions of the studied metals in  $\text{mg kg}^{-1}$  along the collected cores are presented in Figures A1–A15 (Appendix  
203 A). In cases of coarse-grained cores MOT13A, MOT16, UN4, the concentrations in the total sediment (calculated by the  
204 corresponding values in both fractions) are depicted. Table A2 (Appendix A) presents the ratios of eight heavy metals to Al in  
205 the surface and deeper sediment layer of the collected cores. The ratios presented for the cores MOT13A, MOT16, UN4 are  
206 calculated by the results in the corresponding fine-grained sediments. The vertical profiles of metal to aluminum ratios (in fine  
207 grained sediments) along the collected cores, are also given in Figures A1–A15 (Appendix A).

208 Table 4 summarizes the concentrations of eight heavy metals in the surface and deeper sediment layer of the collected cores.  
209 For the sake of direct comparison in the cases of cores MOT13A, MOT16, UN4 the fine grained concentrations are presented  
210 in Table 4. The sediments at the deeper parts of West Saronikos (cores UN6, UN6A and UN11) present elevated concentrations  
211 of Al, Fe, Pb and Zn. The sediments of UN11 are also particularly enriched in Mn. On the contrary the values of Cr and Ni are  
212 elevated in cores MOT13A, MOT16 and MOT16A.

Table 3. Concentrations of metals (in mg Kg<sup>-1</sup>), organic and inorganic carbon content in the two sediment fractions of coarse-grained cores (MOT13A, MOT16, UN4).

| Variable/Core       | MOT13A        |                 | MOT16         |                 | UN4           |                 |
|---------------------|---------------|-----------------|---------------|-----------------|---------------|-----------------|
|                     | fine fraction | coarse fraction | fine fraction | coarse fraction | fine fraction | coarse fraction |
| % TOC               | 0.64-2.80     | 0.26-0.45       | 0.37-2.70     | 0.15-0.46       | 0.65-0.94     | 0.43-0.58       |
| % CaCO <sub>3</sub> | 22-23         | 27-30           | 21-23         | 18-22           | 26-29         | 32-36           |
| Al                  | 10561-18387   | 6615-9226       | 21677-28939   | 10610-18538     | 23271-34246   | 10449-19765     |
| Cr                  | 390-651       | 333-486         | 322-374       | 306-517         | 113-133       | 71.6-115        |
| Ni                  | 293-411       | 220-302         | 314-573       | 424-697         | 139-187       | 78.0-140        |
| Fe                  | 19878-21153   | 17430-20643     | 24130-31694   | 32265-36080     | 14149-17126   | 13501-17931     |
| Mn                  | 429-476       | 326-386         | 471-530       | 435-484         | 317-366       | 174-238         |
| Cu                  | 17.1-18.8     | 8.9-11.8        | 16.7-22.6     | 6.7-14.8        | 15.1-23.6     | 9.7-13.4        |
| Pb                  | 18.0-30.7     | 14.8-21.0       | 9.1-28.0      | 8.3-31.9        | 11.2-31.2     | 9.3-27.3        |
| Zn                  | 39.3-51.8     | 31.0-45.6       | 39.8-53.7     | 31.5-50.9       | 38.9-59.2     | 30.3-50.3       |

216

217

218

219

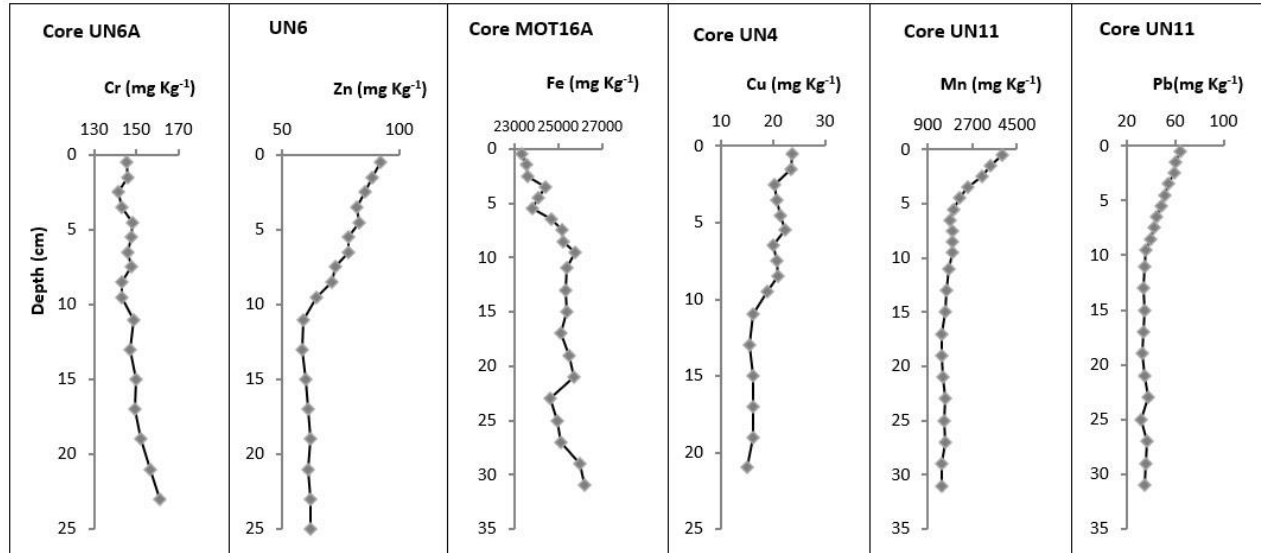
Table 4. Concentrations in mg Kg<sup>-1</sup> of metals in the surface and the deeper sediment layer of cores. The concentrations at coarse-grained cores MOT13A, MOT16, UN4 refer to the fine sediment fraction (f < 63µm).

| Core   | Layer (cm) | Al    | Cr  | Ni  | Fe    | Mn   | Cu   | Pb   | Zn   |
|--------|------------|-------|-----|-----|-------|------|------|------|------|
| MOT13A | 0-1        | 10561 | 651 | 411 | 20988 | 476  | 18.2 | 26.1 | 49.6 |
|        | 10-12      | 14673 | 407 | 383 | 21153 | 444  | 18.1 | 22.5 | 44.6 |
| MOT16A | 0-1        | 27009 | 280 | 375 | 23315 | 578  | 22.6 | 20.4 | 48.3 |
|        | 30-32      | 30070 | 256 | 382 | 26179 | 562  | 22.1 | 28.1 | 44.1 |
| UN5    | 0-1        | 32705 | 199 | 305 | 25534 | 635  | 27.4 | 42.7 | 74.5 |
|        | 30-32      | 37885 | 223 | 320 | 29170 | 520  | 26.0 | 24.7 | 57.5 |
| MOT16  | 0-1        | 21677 | 369 | 377 | 25816 | 530  | 22.6 | 28.0 | 53.7 |
|        | 18-20      | 23807 | 348 | 401 | 29752 | 482  | 16.9 | 9.1  | 40.4 |
| UN6    | 0-1        | 43264 | 142 | 253 | 27301 | 954  | 36.7 | 52.9 | 92.1 |
|        | 24-26      | 44547 | 153 | 274 | 29345 | 707  | 28.5 | 32.5 | 62.4 |
| UN6A   | 0-1        | 39314 | 146 | 187 | 21838 | 570  | 26.3 | 38.4 | 73.8 |
|        | 22-24      | 41303 | 161 | 209 | 23827 | 513  | 25.4 | 38.7 | 58.7 |
| UN4    | 0-1        | 34246 | 132 | 162 | 15762 | 358  | 23.6 | 26.1 | 52.1 |
|        | 20-22      | 31706 | 113 | 160 | 17112 | 365  | 15.1 | 12.0 | 40.3 |
| UN11   | 0-1        | 54626 | 142 | 230 | 32177 | 3925 | 49.7 | 63.9 | 110  |
|        | 30-32      | 48186 | 163 | 217 | 31573 | 1459 | 37.3 | 35.1 | 71.4 |

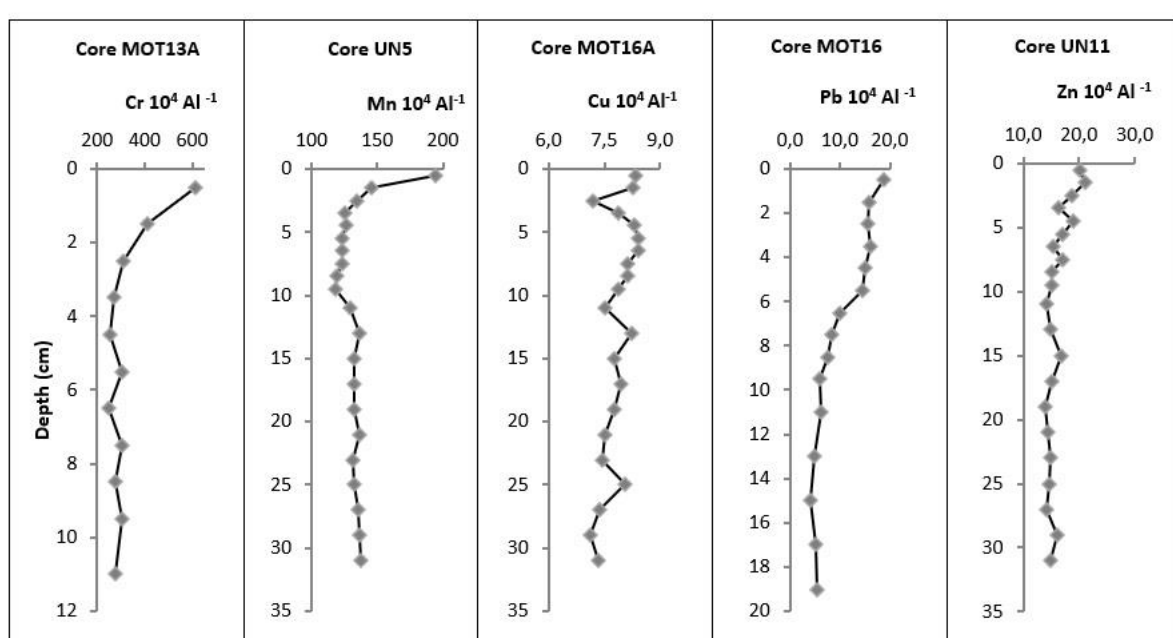
222

The vertical distributions of Al (Fig. A1) for the total sediment (both fractions) present minimal variation. The down-core variability of Al is lower than 10 %, in the finer sediments (MOT16A, UN5, UN6, UN6A and UN11) and between 10-15 % in the coarser sediments (MOT13A, MOT16 and UN4). In the surface layer (0-1cm) of cores MOT13A and UN5 there is a sharp decrease of Al content. Furthermore, the average aluminum content (16709mgKg<sup>-1</sup>) at the top 6cm of core MOT16 is statistically lower (two-sided t-test, p<0,05) than the corresponding average content in the layers below (20477mgKg<sup>-1</sup>). On the contrary, at the top 12cm of core UN11 aluminum (average 52714mgKg<sup>-1</sup>) is increased (two-sided t-test, p<0,05) compared to the deeper layers (average 48621 mgKg<sup>-1</sup>). The other so-called lithogenic metals (Cr, Ni, Fe, Mn) generally present uniform vertical profiles with minimal variability, mostly below 10 % (Figures A2-A9). However, Cr, Ni, Fe and Mn in the surface sediments of MOT13A present an increasing trend, that remains pronounced after normalization to Al in the muddy fraction at the top 0-1cm and is concurrent with the 2-fold decrease of Al content. The vertical profiles of Cr and normalized Cr/Al in UN11 indicate a decrease of Cr in the upper sediment layers. This decrease is confirmed statistically and the average Cr (148mgKg<sup>-1</sup>) and Cr/Al (28,0) values of the top 12cm are lower than the corresponding in the deeper layers (155 mgKg<sup>-1</sup> and 32,0, respectively). The same trend of decrease in the top 0-1cm is seen in the normalized profiles of Fe, Ni and Mn in the fine-grained sediment fraction of core UN4. The average concentrations of Fe, Mn, and Ni in the top 12cm of UN11 are statistically higher than the corresponding in the deeper layers. The most pronounced difference is calculated for Mn, where the average upper layer content is 2396 mgKg<sup>-1</sup> while the deeper layer content is 1527 mgKg<sup>-1</sup>. The same applies to Mn/Al ratio in UN11 but not to the ratios of Fe/Al and Ni/Al which are seemingly lower in the upper layers like Cr/Al but statistically equal. The down-core variability of Mn in all stations, except UN4, is typical of shelf sediments, with high surficial Mn concentrations and Mn/Al ratios that diminish with depth

242 Figure 3 presents selected vertical profiles of Mn and Pb along core UN11 and those of Cr, Fe, Cu, Zn at stations UN6A,  
 243 MOT16A, UN4, UN6, respectively. Figure 4 presents selected vertical distributions of metal to Al ratios at cores MOT13A,  
 244 UN5, MOT16A, MOT16 and UN11. The concentrations and ratios presented in Figures 3 and 4 refer to the muddy fraction of  
 245 the sediments in the cases of the coarse-grained cores (MOT13A, MOT16, UN4).  
 246



247  
 248 **Figure 3: Vertical profiles of Cr, Fe, Cu, Zn at the muddy sediments of cores UN6A, MOT16A, UN4, UN6 respectively and Mn, Pb**  
 249 **250 along core UN11.**



251  
 252 **Figure 4: Vertical distributions of ratios to Al at cores MOT13A, UN5, MOT16A, MOT16 and UN11 of northwest Saronikos Gulf**  
 253 **(profiles for MOT13A and MOT16 depict ratios calculated for the muddy fraction).**

254  
 255 The concentrations of Cu, Pb and Zn as well as the normalized profiles (Fig. A10–A15) show a constant decrease over depth  
 256 to background levels. That tendency is less pronounced with no statistical difference between upper and deeper sediment layers  
 257 in very few cases and particularly for Cu (MOT13A, MOT16, MOT16A), Cu/Al (MOT13A), Pb (MOT13A, MOT16A), Pb/Al  
 258 (MOT16A) and Zn (MOT16A). In all remaining cores the concentrations of Cu, Pb and Zn and the ratios to aluminum in the  
 259 upper sediment layers (above 10cm) are statistically higher than the corresponding in the deeper layers.

## 4.2 Horizontal distributions

261 Figure 5 presents the horizontal distributions of heavy metals in the surface sediments (0-1 cm) of the study area. In cases of  
 262 coarse surface sediments of MOT13A, MOT16, UN4, the concentrations of total sediment fraction (sand and mud) were used.  
 263 The concentrations of Al, Fe, Mn, Cu, Pb and Zn are plotted increased from the northeast to the southwest area of West  
 264 Saronikos Gulf. On the other hand, the concentrations of Fe, Cr and Ni at the north part appear higher than those at the south  
 265 area.

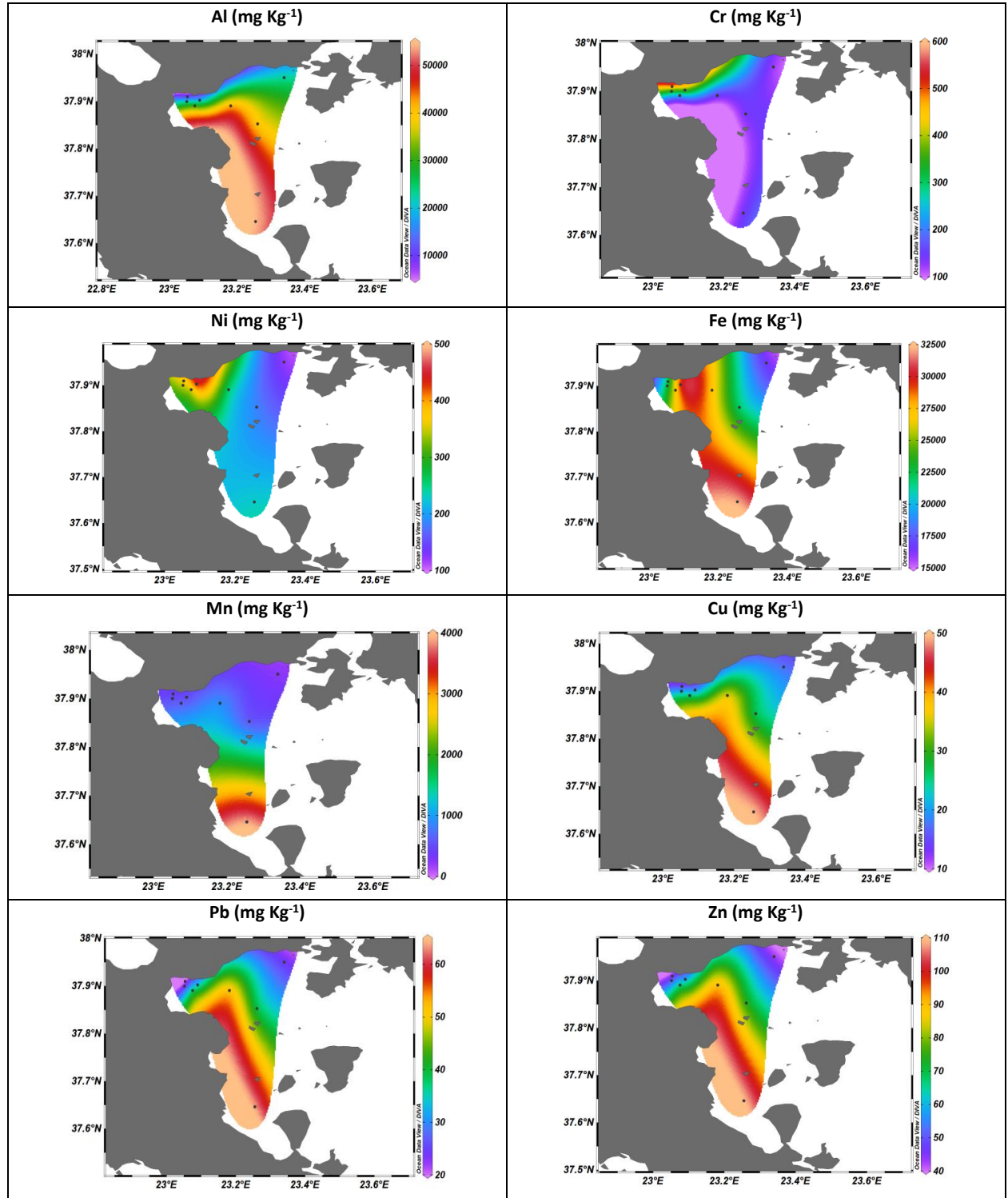


Figure 5: The horizontal distributions of heavy metals in the surface sediments of West Saronikos Gulf. In cases of coarse surface sediments of stations MOT13A, MOT16, UN4, the concentrations of the total sediment (sand and mud) were used.

272 In order to corroborate the above plots and produce solid statistical comparisons for the metal concentrations between stations  
273 the average values and standard deviation from the results of the top 5 cm were calculated and examined used the IBM-SPSS  
274 Statistics 2020 software. In most cases of metals and stations the 5 value groups followed the normal distribution therefore the  
275 parametric One-Way Anova test was first applied. But since some cases did not follow the normal distribution non-parametric  
276 tests (Kruskal-Wallis for multiple groups and Mann-Whitney / Kolmogorov-Smirnov for two groups) were also applied to  
277 corroborate the statistical comparison outcome. The results summary is the following:

278 Al: UN11 >> UN6 = UN6A > UN5 > MOT16A > UN4 = MOT16 >> MOT13A  
279 Fe: UN11 = MOT16 > UN6 = UN5 > MOT16A > MOT13A = UN6A > UN4  
280 Mn: UN11 >> UN6 > MOT16A = UN6A = UN5 = MOT16 > MOT13A > UN4  
281 Cr: MOT13A = MOT16 > MOT16A > UN5 > UN6A = UN11 = UN6 > UN4  
282 Ni: MOT16 > MOT16A > UN5 = MOT13A = UN6 > UN11 > UN6A > UN4  
283 Cu: UN11 > UN6 = UN5 > UN6A > MOT16A > UN4 = MOT16 > MOT13A  
284 Pb: UN11 = UN6 > UN5 = UN6A > UN4 = MOT16 > MOT16A = MOT13A  
285 Zn: UN11 > UN6 > UN5 = UN6A > MOT16 = UN4 = MOT16A = MOT13A.

## 286 5 Discussion

### 287 5.1 Geochemical findings and element interrelations

288 The spatial grain size distribution falls into an expected pattern with coarser sediments closer to the coastline (stations  
289 MOT13A, MOT16, UN4) and finer sediments in the more remote and deeper stations MOT16A, UN5, UN6, UN6A, UN11.  
290 The observed spatial variability of TOC with higher content in the predominantly muddy cores is expected since fine-grained  
291 sediments are known to contain elevated levels of organic material compared to coarse-grained sediments (Salomons &  
292 Forstner, 1984). The pronounced increase of TOC in the muddy sediments of station MOT16 (top 6cm) could be attributed to  
293 the treated wastewater effluents of the refinery which are discharged in the general vicinity of this station (Paraskevopoulou;  
294 2009). The two deep stations UN6 (200m at Megara basin) and UN11 (440m at Epidavros basin) present the highest TOC  
295 content. It has been stipulated that suspended matter from eastern Saronikos basin, which is affected by more pronounced  
296 polluting activities is transported below the thermocline to the west basin (Psyllidou-Giouranovits and Pavlidou, 1998;  
297 Kontoyannis, 2010). This could explain the gradual increase of TOC content in the more recently deposited upper layers of  
298 sediment.

299 Fine-grained sediments are known to contain abundant geochemical phases, such as clay minerals, organic material and Fe-  
300 Mn oxy-hydroxides with high affinity for trace metals due to increased surface adsorption and ionic attraction. Thus, the  
301 elevated levels of Al and the so-called anthropogenic metals (Cu, Pb, Zn) in the muddy sediments of the study area can be  
302 attributed to the predominant occurrence of aluminum-rich aluminosilicate and clay minerals in fine-grained sediments and  
303 their concurrent efficacy to bind or sorb trace metals (Barjy et al., 2020; Karageorgis et al., 2005; Salomons & Forstner, 1984).  
304 In contrast Cr and Ni which are also regarded as lithogenic elements along with Al, present a different distribution and are  
305 elevated in the coarser near-shore sediments of cores MOT13A, MOT16 and MOT16A. This can be attributed to the existence  
306 of ultrabasic rocks in the coastal Susaki area, in which, these metals are abundant (Kelepertsis et al., 2001). In the case of Fe  
307 and Mn the lower contents at station UN4 can be attributed to the coarser sediments and the different geological setting with  
308 absence of ultrabasic rocks.

309 The minimal depth variations observed at the vertical distributions of major (Al) and lithogenic elements (Fe, Cr, Ni) in the  
310 study area are anticipated because of their terrigenous origin (Nolting et al., 1999; Karageorgis et al., 2005;), however some  
311 of the discrepancies identified in specific cores cannot be readily explained due to lack of data for other elements such as Ti,  
312 Si and Ca.

313 The down-core variability of Mn in all stations, except UN4, is typical of shelf sediments, with high surficial Mn concentrations  
314 that diminish with depth, as reducing conditions develop. These variations are largely independent of lithological or carbonate  
315 content fluctuations, and are attributed solely on the respiration of organic carbon and the redox-cycle of Mn (Karageorgis et  
316 al., 2005; Sundby, 2006). The Mn enrichment is far more pronounced in the surface sediments of station UN11 and subtle in  
317 the other muddy cores. In station UN11 the bottom waters have been hypoxic or near anoxic since the mid 90's (Kontoyiannis,  
318 2010; Paraskevopoulou et al., 2014). A possible explanation is that the slow diffusion of dissolved oxygen from the more  
319 oxidizing overlying waters and the upward diffusion of dissolved Mn (II) from the pore water of anoxic surface sediments to  
320 the sediment/water interface (Ozturk, 1995), cause the oxidation of dissolved Mn (II) and its precipitation as Mn (IV) oxides  
321 (Pohl and Hennings, 1999). The Mn enrichment in the surface layers of UN11 resembles concentrations in sediments from  
322 suboxic parts of the Black Sea (Kiratli & Ergin, 1996; Chen et al., 2022).

323 The normalized profiles of Cu, Pb and Zn exhibit statistically higher metal ratios in the upper layers of the cores, which is a  
324 typical indication of the effect of modern pollution sources to recently deposited sediments in contrast to pre-industrial  
325 deposition of the deeper layers (Karageorgis. et al., 2005).

326 The concentrations of Al, Fe, Mn, Cu, Pb and Zn are increased from the northeast to the southwest area of West Saronikos  
327 Gulf generally following the distribution of muddy sediments. The opposite increase of Cr and Ni to the north of the study  
328 area is attributed to the ultrabasic geological substrate of the Susaki coastal area. The exception of increased Fe concentrations  
329 in one of the northern sandy cores (MOT16) can also be attributed to the geology of the coastal region (Kelepertsis et al.,  
330 2001).

331 Spearman's correlation analysis was carried out to determine the relationships between heavy metals and percentages of total  
332 organic carbon (TOC) and carbonates in sediments of the collected cores. The concentrations of metals and the percentages of  
333 organic and inorganic carbon used for the analysis correspond to the fine fraction in the sediments of stations MOT13A,  
334 MOT16, UN4. Spearman's correlation coefficients are presented in Table A3 (appendix A) and Fig. A16 (appendix A).

335 Al is highly correlated ( $r > 0.5$ ,  $p < 0.05$ ) with Fe, Mn, Cu, Pb and Zn, which probably indicates an association between these  
336 metals in the form of metal-clay complexes of continental origin (Barjy et al., 2020). On the other hand, there is a negative  
337 correlation of Al with Cr and Ni.

338 Cr is highly correlated with Ni, but both of them show negative correlation with Cu, Pb and Zn, which can be attributed to  
339 their different origin (Barjy et al., 2020) and poor correlation with Mn. Cr shows poor correlation with Fe, as well. The strong  
340 correlation between Cr and Ni can be observed at sediments of the northwest part, too.

341 Fe, Mn, Cu, Pb and Zn show positive correlation with each other. Cu, Pb and Zn are highly correlated with each other ( $r > 0.5$ ,  
342  $p < 0.05$ ), which can be observed at sediments of the northwest part, too, suggesting that they have a common origin and  
343 identical behavior during transport in the marine environment (Barjy et al., 2020).

344 The % TOC content presents moderate correlation with Al, Cu, Pb and Zn and negative correlation with Cr, Ni and %  
345 carbonates. Moreover, it shows poor correlation with Fe and Mn. Finally, the percentage of carbonates content presents  
346 negative correlation with all metals.

347

## 348 **5.2 Enrichment Factors**

349 The Enrichment Factors (EF) are used to distinguish between metals originating from anthropogenic activities and from natural  
350 processes, assessing the degree of anthropogenic effect. Equation (1) was used for the calculations of EFs, where  $C_x$  is the  
351 concentration of the analyzed metal and  $C_{EN}$  is the concentration of the normalizing element. Al was used as the reference  
352 element.

353  $EF = (C_x/C_{EN})_{sample}/(C_x/C_{EN})_{background}$  (1)

354 In Table 5, the categories of contamination according to the Enrichment Factor are presented (Diamantopoulou et al., 2019;  
 355 Sutherland, 2000). In general, EFs use concentrations normalized to Al to account for the heterogeneity of the samples due to  
 356 differences in texture and organic content (Gredilla et al., 2015).

357

358 **Table 5. The categories of pollution according to the Enrichment Factor.**

| EF       | Contamination Degree                                     |
|----------|--|
| < 2      | Depletion to minimal enrichment- no or minimal pollution |
| 2 to 5   | Moderate enrichment- moderate pollution                  |
| 5 to 20  | Significant enrichment- significant pollution            |
| 20 to 40 | Very high enrichment- very strong pollution              |
| >40      | Extreme enrichment- extreme pollution                    |

359

360 Table 6 presents the Enrichment Factors of the surface sediments (0-1 cm) that were calculated based on the measured  
 361 concentrations of heavy metals. The EFs were calculated at the fine fraction ( $f < 63\mu\text{m}$ ) of sediments of cores MOT13A,  
 362 MOT16, UN4. Most metals present minimal to moderate enrichment in almost all the cores analysed. Moderate enrichment is  
 363 found for Cr, Ni, Mn and Pb in core MOT13A, Mn in UN11, and finally for Pb in UN5 and MOT16.

364

365 **Table 6. Enrichment Factors of the surface sediments (0-1cm) of the study area. In cases of stations MOT13, MOT16, UN4, the EFs  
 366 were calculated at the fine surface sediment fraction ( $f < 63\mu\text{m}$ ).**

| Core     | EF Cr | EF Ni | EF Fe | EF Mn | EF Cu | EF Pb | EF Zn |
|----------|-------|-------|-------|-------|-------|-------|-------|
| MOT 13 A | 3.09  | 2.07  | 1.92  | 2.07  | 1.94  | 2.24  | 2.14  |
| MOT 16A  | 1.36  | 1.22  | 1.10  | 1.27  | 1.27  | 0.90  | 1.36  |
| UN 5     | 1.20  | 1.28  | 1.17  | 1.64  | 1.42  | 2.32  | 1.74  |
| MOT 16   | 1.28  | 1.14  | 1.05  | 1.33  | 1.61  | 3.71  | 1.60  |
| UN6      | 0.98  | 0.98  | 0.99  | 1.43  | 1.36  | 1.73  | 1.57  |
| UN 6A    | 1.00  | 0.99  | 1.01  | 1.23  | 1.15  | 1.09  | 1.39  |
| UN 4     | 1.00  | 0.87  | 0.79  | 0.84  | 1.34  | 1.86  | 1.11  |
| UN11     | 0.68  | 0.82  | 0.79  | 2.09  | 1.04  | 1.42  | 1.20  |

368

### 369 **5.3 Sediment Quality Guidelines**

370 Sediment Quality Guidelines (SQG) of effects range low (ERL) and effects range median (ERM) are used to assess the level  
 371 of toxicity of metals in the surface sediments. Metal concentrations below the ERL value, indicate that effects on biota are  
 372 rarely observed. Concentrations above the ERL but below the ERM, occasionally affect the biota and concentrations above  
 373 the ERM frequently affect the biota. The ERL and ERM guideline values for trace metals ( $\text{mgKg}^{-1}$ , dry wt) and percent  
 374 incidence of biological effects in concentrations ranges defined by the two values are presented in Table 7 (Long et al., 1995).

375

376 **Table 7. ERL and ERM guideline values for trace metals ( $\text{mgKg}^{-1}$ , dry wt) and percent incidence of biological effects in concentration  
 377 ranges defined by the two values.**

| Metal | ERL ( $\text{mg kg}^{-1}$ ) | ERM ( $\text{mg kg}^{-1}$ ) | Percent incidence of effects |         |      |
|-------|-----------------------------|-----------------------------|------------------------------|---------|------|
|       |                             |                             | <ERL                         | ERL-ERM | >ERM |
| Cr    | 81                          | 370                         | 2.9                          | 21.1    | 95.0 |
| Cu    | 34                          | 270                         | 9.4                          | 29.1    | 83.7 |
| Pb    | 46.7                        | 218                         | 8.0                          | 35.8    | 90.2 |
| Ni    | 20.9                        | 51.6                        | 1.9                          | 16.7    | 16.9 |
| Zn    | 150                         | 410                         | 6.1                          | 47.0    | 69.8 |

379

380 In this study, the concentrations of heavy metals at the surface sediments were compared with the ERL and ERM criteria. For  
 381 cores MOT13A, MOT16, UN4, the concentrations in the total sediment (< 1mm) were used. The concentrations of Cr in the  
 382 surface sediments of cores UN4, UN5, MOT16A, UN6, UN6A and UN11 are higher than the ERL value ( $81 \text{ mg Kg}^{-1}$ ) but  
 383 below the ERM value ( $370 \text{ mg Kg}^{-1}$ ) and the values at surface sediments of MOT13A and MOT16 are higher than the ERM

384 value. The concentrations of Ni at the surface sediments of the collected cores are higher than the ERM value (51.6 mg Kg<sup>-1</sup>)  
385 and as a result, they frequently affect the biota (Long et al., 1995; Hahlakakis et al., 2012).  
386 The concentrations of Cu and Pb at surface sediments of stations MOT13A, MOT16A, UN4, UN5, MOT16 and UN6A, are  
387 below the ERL values (34 mg Kg<sup>-1</sup> for Cu and 46.7 mg Kg<sup>-1</sup> for Pb), which indicates that effects on biota are rarely observed.  
388 On the other hand, the concentrations at surface sediments of cores UN6 and UN11 are higher than the ERL values but below  
389 the ERM values (270 mg Kg<sup>-1</sup> for Cu and 218 mg Kg<sup>-1</sup> for Pb), which means that they can occasionally affect biota . The  
390 concentrations of Zn are below the ERL (150 mg Kg<sup>-1</sup>) value and the ERM value (410 mg Kg<sup>-1</sup>), which indicates that effects  
391 on biota are rarely observed (Long et al., 1995; Hahlakakis et al., 2012).

#### 392 5.4 Mean effects range medium quotients

393 The mean effects range medium quotient (mERMq) is an index that is used to evaluate the possible biological effects of the  
394 coupled toxicity of all heavy metals in the surface sediments (Gredilla et al., 2015). Briefly, mERMq's were calculated by  
395 dividing the average concentration of each metal at the top 9cm, by its respective ERM (effects range median), to obtain the  
396 corresponding sediment quality guideline quotient (ERMq). Following this, mERMq's for each core were obtained as the  
397 average of ERMqs previously calculated. ERMqs indicate the pollutant concentration above which effects are expected to be  
398 frequent and have been only defined for very toxic elements (Gredilla et al., 2015).

399 In this study, Cr, Ni, Cu, Pb and Zn were considered in our calculations and the results are depicted in Table 8. In cases of  
400 cores MOT13A, MOT16, UN4, the concentrations of the total sediment (< 1mm) were used for the calculation of mERMq.  
401 Values of mERMq in the ranges of 0.0-0.1, 0.1-0.5, 0.5-1.5 and >1.5 correspond to the following probabilities of toxicity: 9  
402 % (non-toxic), 21 % (slightly toxic), 49 % (moderately toxic) and 76 % (highly toxic), respectively (Gredilla et al., 2015). The  
403 mERMq values obtained for the sediments varied from 0.62 to 2.00, which means that the sediments are moderately or highly  
404 toxic.

405 The concentrations of Cr, Ni, Cu, Pb, Zn in sediments of cores MOT13A, UN5, UN6, UN6A, UN4 and UN11 are moderately  
406 toxic and in sediments of MOT16A and MOT16 highly toxic. The concentrations of Cu, Pb, Zn in sediments of cores  
407 MOT13A, MOT16A, MOT16, UN4 are non-toxic, with mERMq ranging from 0.08 to 0.10 and those in sediments of UN5,  
408 UN6, UN6A, UN11 are slightly toxic, with mERMq range 0.16-0.21.

409

410 **Table 8. MERMqs values calculated for the surface sediments (0-9 cm) of the collected cores of West Saronikos Gulf, by dividing  
411 the average concentration (mg Kg<sup>-1</sup>) of each metal (Cr, Ni, Cu, Pb, Zn) by its respective ERM (mg Kg<sup>-1</sup>). In cases of cores MOT13A,  
412 MOT16, UN4, the concentrations of total sediment (< 1mm) were used.**

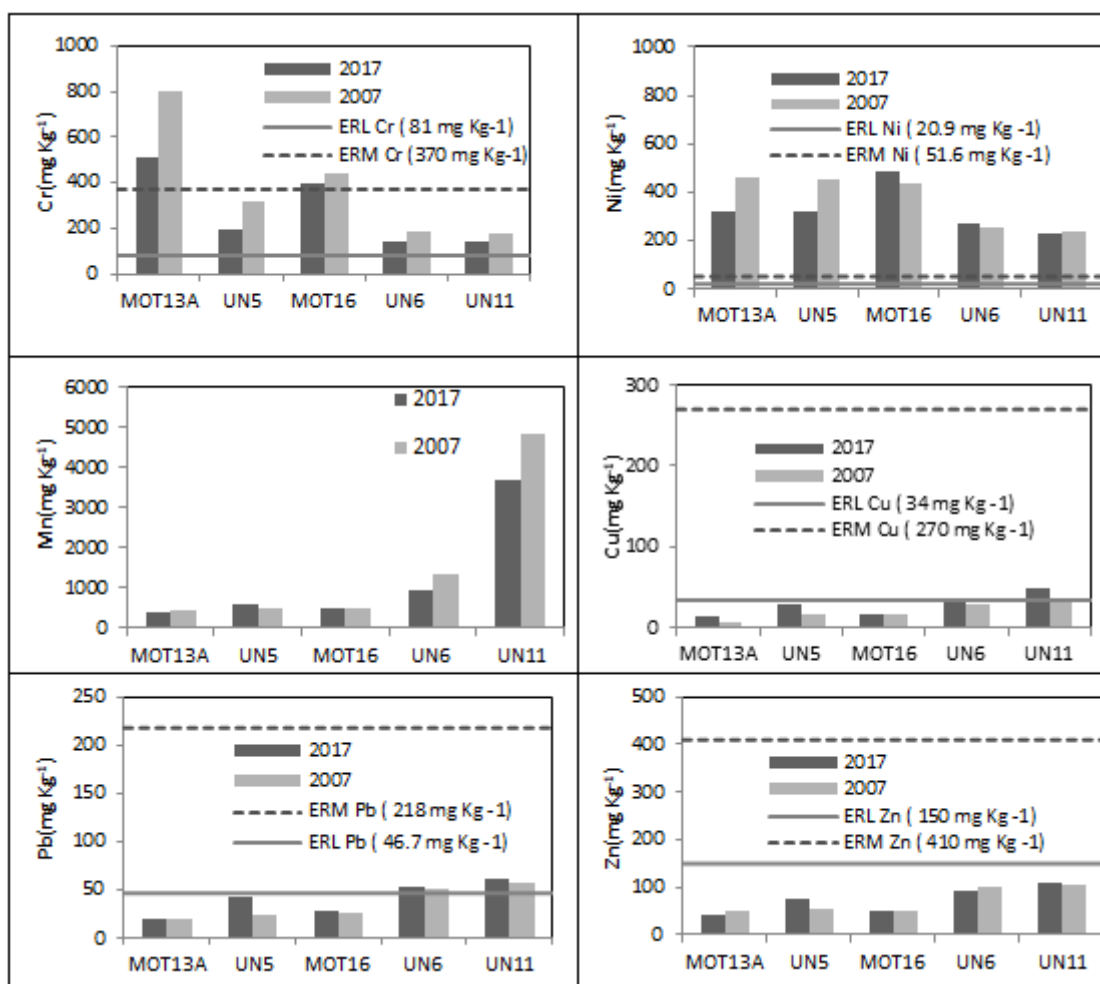
| Core   | mERMq (average) | toxicity of sediments |
|--------|-----------------|-----------------------|
| MOT13A | 1.46            | Moderately toxic      |
| MOT16A | 1.69            | Highly toxic          |
| UN5    | 1.46            | Moderately toxic      |
| MOT16  | 2.00            | Highly toxic          |
| UN6    | 1.21            | Moderately toxic      |
| UN6A   | 0.95            | Moderately toxic      |
| UN4    | 0.62            | Moderately toxic      |
| UN11   | 1.09            | Moderately toxic      |

#### 414 5.5 Evolution of marine pollution

415 The total concentrations of eight heavy metals in the surface sediments were compared with those of a similar study ten years  
416 ago (Paraskevopoulou, 2009). In cores MOT13A, MOT16, UN4, the concentrations of the total sediment fraction (<1mm)  
417 were used and the results are depicted in Fig.6. The levels of Cr, Ni and Mn at most sediments, are decreased in 2017, compared  
418

419 to the study of 2007. On the other hand, the levels of Pb and Cu are increased in 2017, compared to the study of 2007. Moreover,  
420 the levels of Zn, at most sediments, are decreased in 2017 compared to the study of 2007.

421



422

423 **Figure 6: Levels of heavy metals in surface sediments of 2017 and 2007 plotted with sediment quality guidelines. For the coarse**  
424 **sediments of stations MOT13A, MOT16, UN4, the concentrations of total sediment (< 1mm) were used.**

425

#### 426 **5.6 Comparison of metal concentrations in West Saronikos Gulf with other areas of Saronikos Gulf**

427 The concentrations of heavy metals in the surface sediments of West Saronikos Gulf from the present study are compared with  
428 data from the other sub-areas of Saronikos. Specifically the data reviewed are: a) from surface sediments collected in Elefsis  
429 Bay (EB), Inner Saronikos Gulf (ISG) and Outer Saronikos Gulf (OSG) during the same sampling of October 2017 and  
430 analyzed in the Laboratory of Environmental Chemistry using the same methodologies (Xarlis; 2018; Vretou,2019) and b)  
431 data from surface sediments in Elefsis Bay (EB), Inner Saronikos Gulf (ISG) and Outer Saronikos Gulf (OSG) from various  
432 samplings conducted by the Hellenic Centre for Marine Research and analyzed by X-ray Fluorescence (Karageorgis et al.,  
433 2020; Karageorgis et al., 2020a). Summary results of this comparative review are provided in Table 9. The location of selected  
434 stations from the other sub-areas of Saronikos are roughly given in Fig. A17 (Appendix). Furthermore, metal concentrations  
435 in sediments from various areas of Greece analyzed by X-ray Fluorescence (Kanellopoulos et al., 2022) were also reviewed.  
436 It is observed that high Al concentrations are recorded at West Saronikos as well as the Outer Gulf, related to the settling of  
437 finer aluminosilicates in deeper waters. Moreover, high values of Al contents at Elefsis Bay (S1 and neighbouring stations,  
438 Fig. A17) are attributed to the terrigenous inputs from ephemeral streams discharging into the bay (Karageorgis et al., 2020).  
439 Cr and Ni contents show maxima in the northwestern stations (MOT13A, MOT16, MOT16A) offshore Susaki, due to the  
440 geological contribution from ophiolite complexes (Kelepertsis et al., 2001). Ni and Cr concentrations throughout the northwest

441 area of Saronikos are higher than the mean background contents (117 mg Kg<sup>-1</sup> for Ni and 142 mg Kg<sup>-1</sup> for Cr) estimated from  
442 sediments sampled at various areas of Greece and similar to concentrations reported for Aliveri Bay and the Asopos river  
443 basin, also related to occurrence of ultrabasic rocks (Kanellopoulos et al., 2022).

444 The concentrations of Mn and Fe are similar throughout the sub-areas of Saronikos Gulf, with the exception of Epidavros  
445 basin, where the maximum values are recorded due to the settling of finer aluminosilicates in deeper waters and possibly the  
446 implications of bottom water hypoxia/anoxia already discussed in previous sections (Kontoyannis, 2010; Karageorgis et al.,  
447 2020).

448

449 **Table 9. Comparison of heavy metals concentrations in mg Kg<sup>-1</sup> between areas of Saronikos Gulf.**

| Area / Stations          | Al              | Cr       | Ni       | Fe              | Mn           | Cu        | Pb        | Zn        | References  |
|--------------------------|-----------------|----------|----------|-----------------|--------------|-----------|-----------|-----------|---|
| West Saronikos           |                 |          |          |                 |              |           |           |           | Present work  |
| MOT13A, MOT16,<br>MOT16A | 5697-<br>27009  | 280-552  | 344-484  | 20740-<br>21191 | 422-578      | 13.5-22.6 | 20.0-30.3 | 44.1-52.1 |   |
| UN5, UN6, UN6A           | 32705-<br>43264 | 142-199  | 187-305  | 21838-<br>27301 | 570-954      | 26.3-36.7 | 38.4-52.9 | 73.8-92.1 |   |
| UN4                      | 22702           | 123      | 123      | 16682           | 270          | 17.5      | 24.5      | 43.6      |   |
| UN11                     | 54626           | 142      | 230      | 32177           | 3925         | 49.7      | 63.9      | 110       |   |
| Outer Saronikos          | 14000-<br>42000 | 81.5-133 | 29.5-106 | 6407-<br>27139  | 293-<br>1159 | 12.8-22.9 | 15.9-58.9 | 32.4-110  | Karageorgis et al.,<br>2020a; Vrettou,2019                  |
| Inner Saronikos          | 2900<br>37700   | 30.7-184 | 9.6-87.1 | 3235-<br>20795  | 61.5-442     | 7.9-68.5  | 8.2-73.6  | 15.2-170  | Karageorgis et al.,<br>2020a; Vrettou, 2019;<br>Xarlis,2018 |
| Psittalia (S7)           | 26780           | -        | 83.2     | 20623           | 239          | 103       | 102       | 251       | Panagopoulou, 2018;<br>Xarlis, 2018                         |
| Elefsis Bay              | 35000<br>61000  | 108-176  | 41.2-119 | 29721-<br>30499 | 282-579      | 32.1-137  | 61.0-171  | 188-521   | Karageorgis et al.,<br>2020a; Xarlis,2018                   |

451

452 The so-called anthropogenic metals Cu, Pb and Zn show maxima at Elefsis Bay, while their concentrations at the other parts  
453 of Saronikos are reported lower. The levels at Epidavros basin (UN11) are the highest among the stations of West Saronikos,  
454 which can be attributed to the transport of pollutants from the eastern basin (Psyllidou-Giouranovits and Pavlidou, 1998;  
455 Dassenakis et al., 2003). However, the West Saronikos levels of Cu, Pb and Zn remain lower than polluted stations of Inner  
456 Saronikos, such as OS2 (near the port of Pireaus) and S7 (Psittalia, outfall of the Athens Waste Water Treatment Plant)  
457 presented depicted in Gig. A17. Furthermore, Cu, Pb and Zn concentrations at Megara and Epidavros basins are similar to  
458 those at surface sediments of Malliakos and Pagassitikos Gulf (Kanellopoulos et al., 2022) and the concentrations found in  
459 most stations of Inner and Outer Saronikos (Karageorgis et al., 2020; Panagopoulou,2018; Vrettou,2019; Xarlis,2018) but  
460 higher than less affected island areas such as Chios Port, Milos and Andros (Kanellopoulos et al., 2022). In general the West  
461 Saronikos sediments, affected by a relatively small industrial zone, are much less contaminated by Zn compared to the  
462 concentrations well above 150 mg Kg<sup>-1</sup> found in specific locations of Elefsis Bay, Inner Saronikos, Thessaloniki Bay, Ierissos  
463 and Lavrio (Karageorgis et al., 2020, Kanellopoulos et al., 2022) with extensive pollution sources such as the Elefsis industrial  
464 zone, Piraeus Port, the Athens Waste Water Treatment Plant outfall, major rivers of Northern Greece and current or historical  
465 mining operations.

## 466 **6 Conclusions**

467 The heavy metal pollution of West Saronikos Gulf has not been sufficiently studied, despite the scientific interest of this area,  
468 in contrast to the numerous studies of the eastern coast. The distribution of metals in the sediment samples of West Saronikos  
469 indicates that the area is enriched in metals from both geological and anthropogenic origins. The concentrations of all metals  
470 (Al, Mn, Cr, Ni, Cu, Pb, Zn) in muddy sediments are higher than those measured in sandy sediments. The cores are fairly  
471 homogeneous, in terms of carbonates and the down-core variability of % TOC, is characterized by high surficial values that  
472 decrease with depth.

473 The Cr and Ni concentrations at the northwest part of the study area are higher than those measured at the southwest area and  
 474 their values are very stable with depth of most sediment cores, which can be attributed to the geological background of the  
 475 adjacent coast. Al, Fe and Mn are increased from the northeast to the southwest part of the study area. The concentrations of  
 476 Al and Fe increase with depth in most cores, while the values of Mn decrease with depth. Generally, concentrations of Fe and  
 477 Mn at surface sediments are affected by oxic and hypoxic conditions and the settling of finer aluminosilicates.  
 478 The vertical distributions of Cu, Pb and Zn present a constant decrease over depth along most cores, which can be attributed  
 479 to their anthropogenic origin. Moreover, their levels at most sediments are higher than those measured ten years ago. Finally,  
 480 the Cu, Pb, Zn concentrations in West Saronikos Gulf surface sediments are comparable with those at Outer Saronikos Gulf  
 481 and lower than those from Inner Saronikos Gulf, Elefsis Bay and other pollution hot spots of Greece, which can be attributed  
 482 to the smaller industrial zone and sparse urbanized settlements of the West Saronikos coast.  
 483 The concentrations of metals that are measured higher than the ERL values and the indication for moderately or highly toxic  
 484 sediments by the calculation of mERMq signify that more research is required, in order to investigate probable effects on the  
 485 marine ecosystem. Continuous monitoring, updating of the results of the present study complemented with detailed  
 486 geochemical analysis for major elements and minerals identification as well as core dating, metal speciation and study of  
 487 bioaccumulation should be conducted, to assess the impacts of heavy metal pollution on the marine environment of West  
 488 Saronikos Gulf.

489 **7 Appendices**

490 **Appendix A**

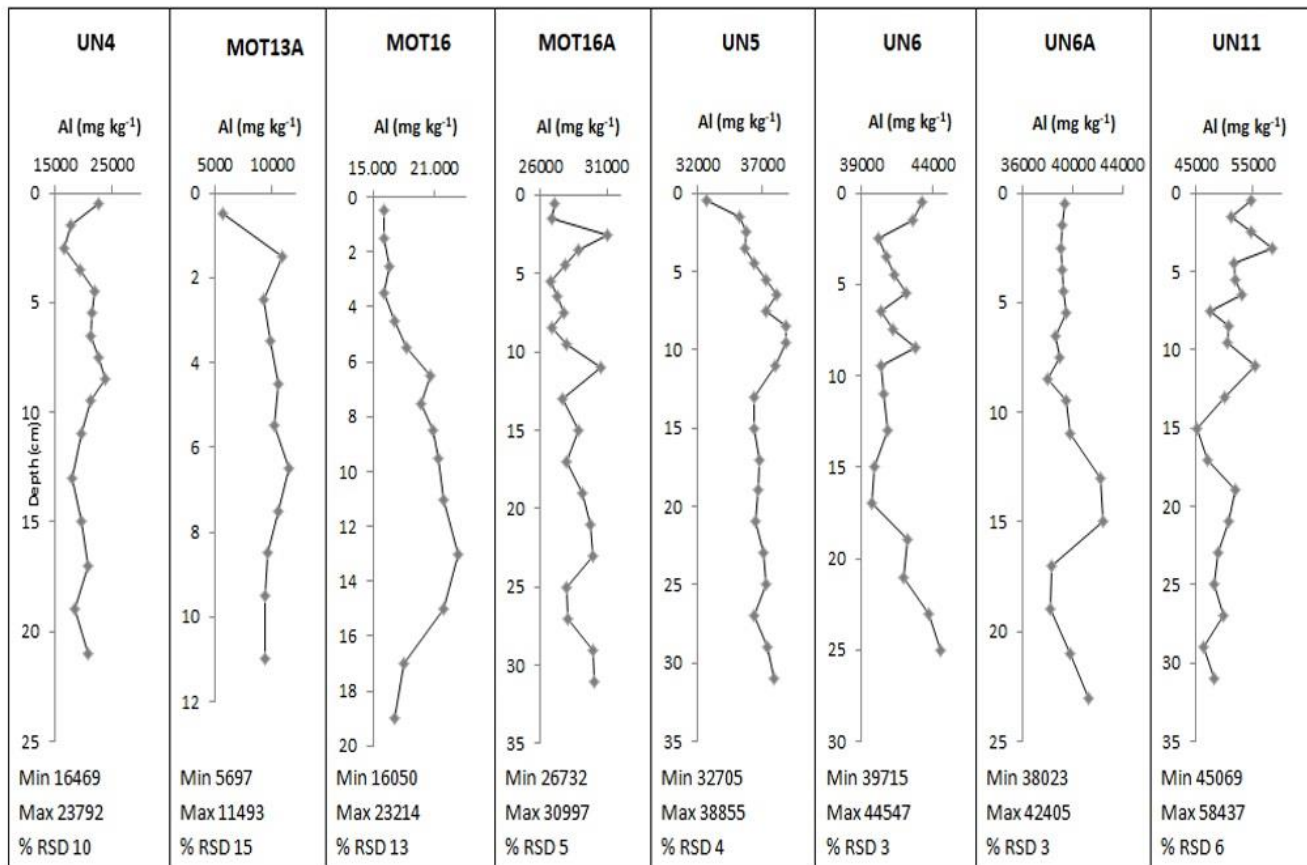
491 **Table A1. Quality control data for total metal analyses.**

| Quality parameter                    | Al      | Cr      | Cu      | Fe      | Mn      | Ni      | Pb      | Zn      |
|--------------------------------------|---------|---------|---------|---------|---------|---------|---------|---------|
| Daily duplicates %RSD (range)        | 0.8-4.6 | 1.2-6.2 | 0.4-6.0 | 0.4-5.1 | 0.2-6.6 | 0.8-9.2 | 1.1-8.2 | 0.5-4.0 |
| Daily duplicates %RSD (average)      | 2.3     | 3.6     | 3.4     | 1.3     | 1.5     | 3.4     | 3.8     | 1.9     |
| %RSD for PACS reproducibility (n=15) | 6.2     | 8.3     | 3.2     | 2.6     | 7.4     | 9.7     | 6.2     | 4.0     |
| Accuracy (% Recovery range)          | 85-106  | 84-114  | 87-96   | 86-95   | 85-113  | 85-115  | 86-109  | 86-99   |
| Accuracy (% Recovery average)        | 96      | 96      | 91      | 89      | 99      | 101     | 95      | 91      |

493  
 494 **Table A2. The ratios of eight heavy metals to Al in surface and deeper layer sediments of the collected cores. In cases of coarse-  
 495 grained sediment cores MOT13A, MOT16, UN4, the ratios in fine sediment fraction ( $f < 63 \mu\text{m}$ ) are calculated.**

| Core     | Layer (cm) | Cr $10^4 \text{ Al}^{-1}$ | Ni $10^4 \text{ Al}^{-1}$ | Fe $\text{Al}^{-1}$ | Mn $10^4 \text{ Al}^{-1}$ | Cu $10^4 \text{ Al}^{-1}$ | Pb $10^4 \text{ Al}^{-1}$ | Zn $10^4 \text{ Al}^{-1}$ |
|----------|------------|---------------------------|---------------------------|---------------------|---------------------------|---------------------------|---------------------------|---------------------------|
| MOT 13 A | 0-1        | 616                       | 389                       | 1.99                | 451                       | 17.3                      | 24.7                      | 46.9                      |
|          | 10-12      | 277                       | 261                       | 1.44                | 303                       | 12.4                      | 15.4                      | 30.4                      |
| MOT 16A  | 0-1        | 104                       | 139                       | 0.86                | 214                       | 8.35                      | 7.55                      | 17.9                      |
|          | 30-32      | 85.0                      | 127                       | 0.87                | 187                       | 7.35                      | 9.35                      | 14.7                      |
| UN 5     | 0-1        | 61.0                      | 93.1                      | 0.78                | 194                       | 8.39                      | 13.1                      | 22.8                      |
|          | 30-32      | 58.9                      | 84.5                      | 0.77                | 137                       | 6.85                      | 6.52                      | 15.2                      |
| MOT 16   | 0-1        | 170                       | 174                       | 1.19                | 244                       | 10.4                      | 12.9                      | 24.8                      |
|          | 18-20      | 146                       | 168                       | 1.25                | 203                       | 7.11                      | 3.81                      | 17.0                      |
| UN6      | 0-1        | 32.7                      | 58.4                      | 0.63                | 220                       | 8.48                      | 12.2                      | 21.3                      |
|          | 24-26      | 34.2                      | 61.6                      | 0.66                | 159                       | 6.41                      | 7.29                      | 14.0                      |
| UN 6A    | 0-1        | 37.0                      | 47.5                      | 0.56                | 145                       | 6.7                       | 9.76                      | 18.8                      |
|          | 22-24      | 39.0                      | 50.6                      | 0.58                | 124                       | 6.14                      | 9.38                      | 14.2                      |
| UN 4     | 0-1        | 38.6                      | 47.4                      | 0.46                | 104                       | 6.9                       | 7.63                      | 15.2                      |
|          | 20-22      | 35.7                      | 50.5                      | 0.54                | 115                       | 4.75                      | 3.80                      | 12.7                      |
| UN11     | 0-1        | 26.1                      | 42.0                      | 0.59                | 719                       | 9.1                       | 11.7                      | 20.2                      |
|          | 30-32      | 33.8                      | 45.1                      | 0.66                | 303                       | 7.75                      | 7.29                      | 14.8                      |

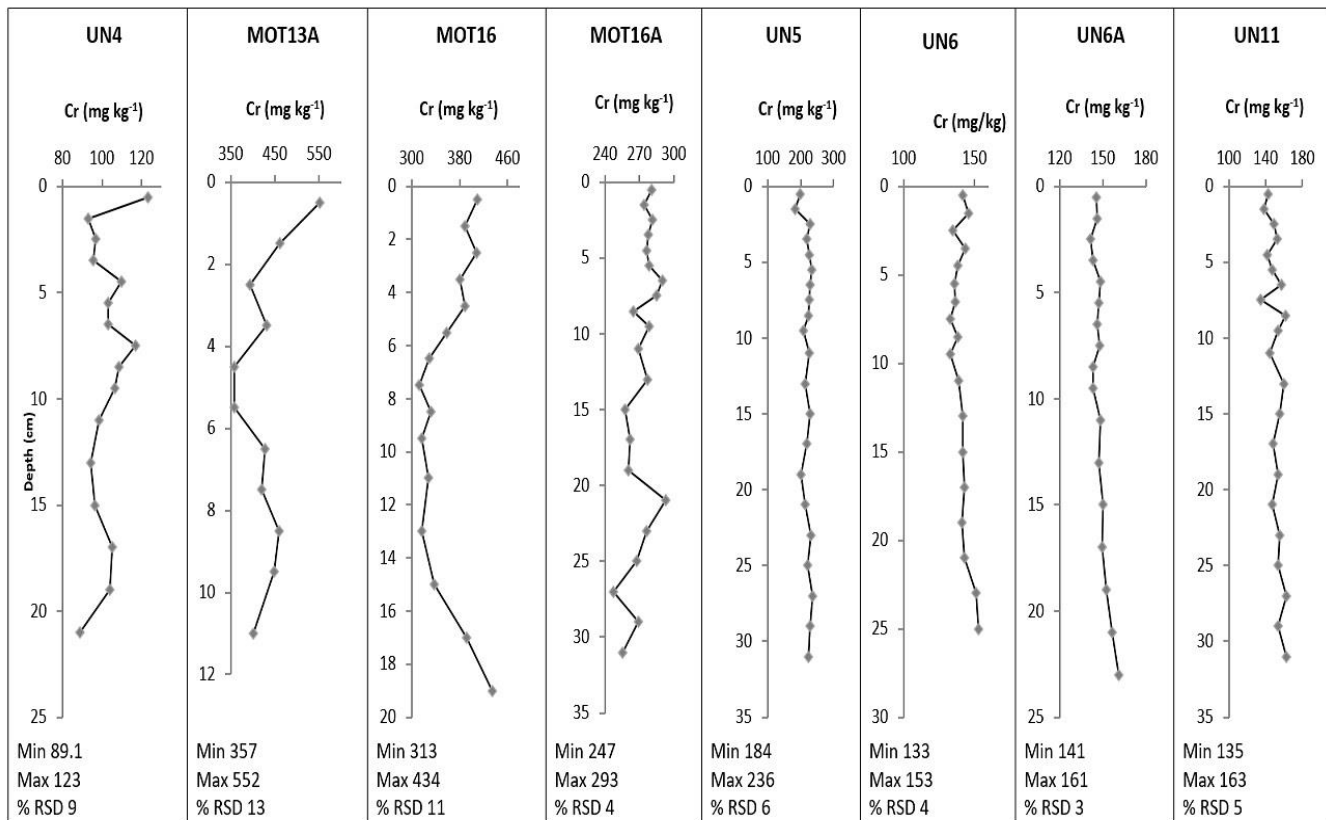
498



499

500  
501

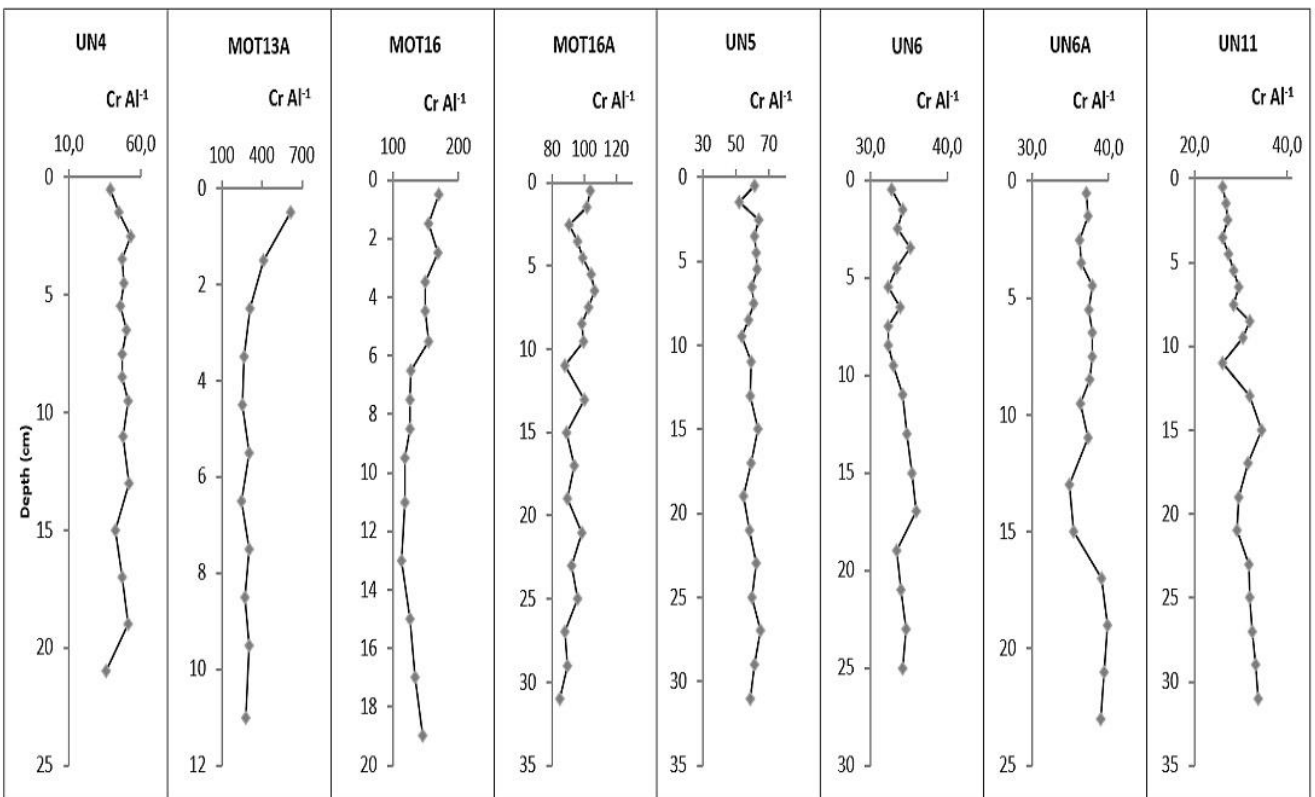
Figure A1: Vertical distributions of Al in  $\text{mg kg}^{-1}$  in sediment cores. The concentrations in coarse cores MOT13A, MOT16, UN4 refer to the total sediment fraction (< 1 mm).



502

503  
504

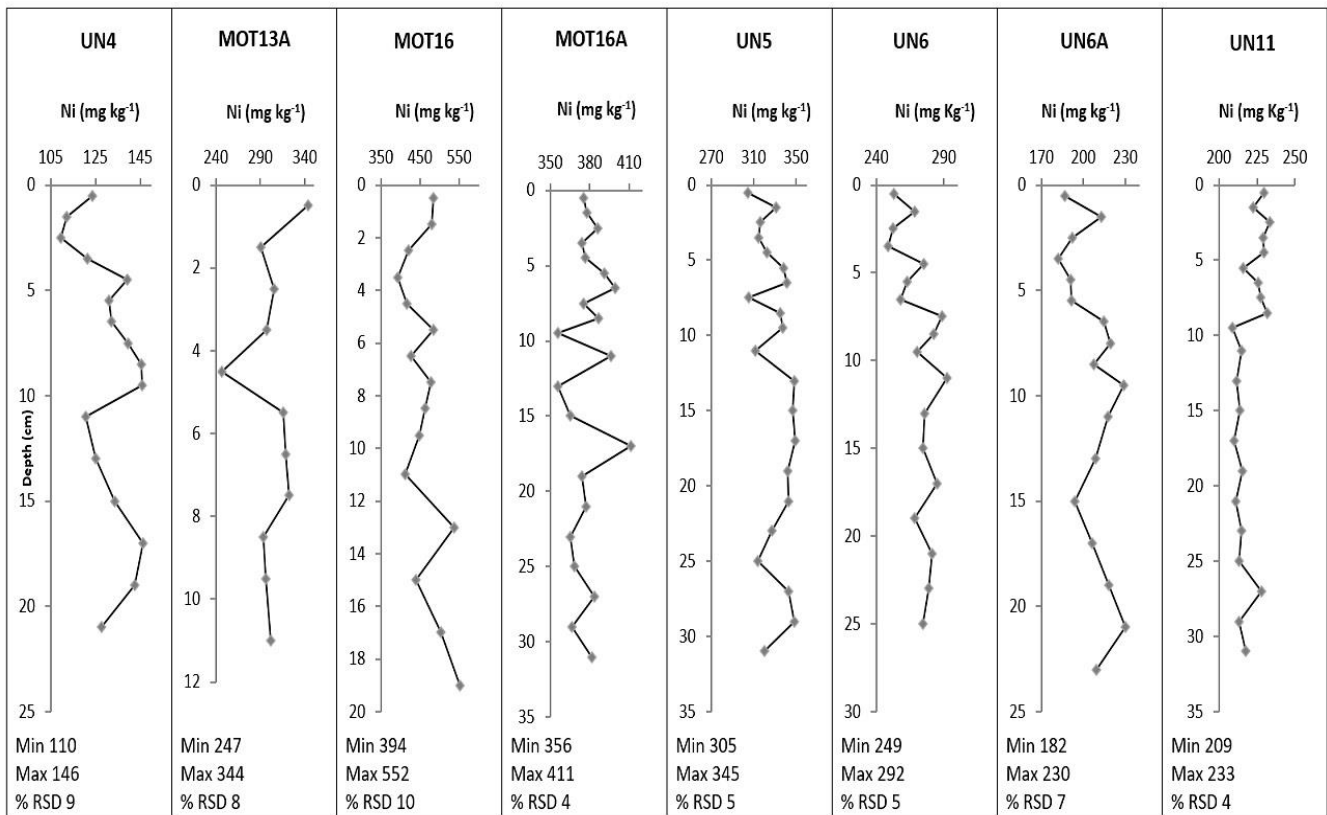
Figure A2: Vertical distributions of Cr in  $\text{mg kg}^{-1}$  in sediment cores. The concentrations in coarse cores MOT13A, MOT16, UN4 refer to the total sediment fraction (< 1 mm).



505

506 **Figure A3: Vertical distributions of Cr Al<sup>-1</sup> × (10<sup>4</sup>) in sediment cores. The ratios in coarse cores MOT13A, MOT16, UN4 are**

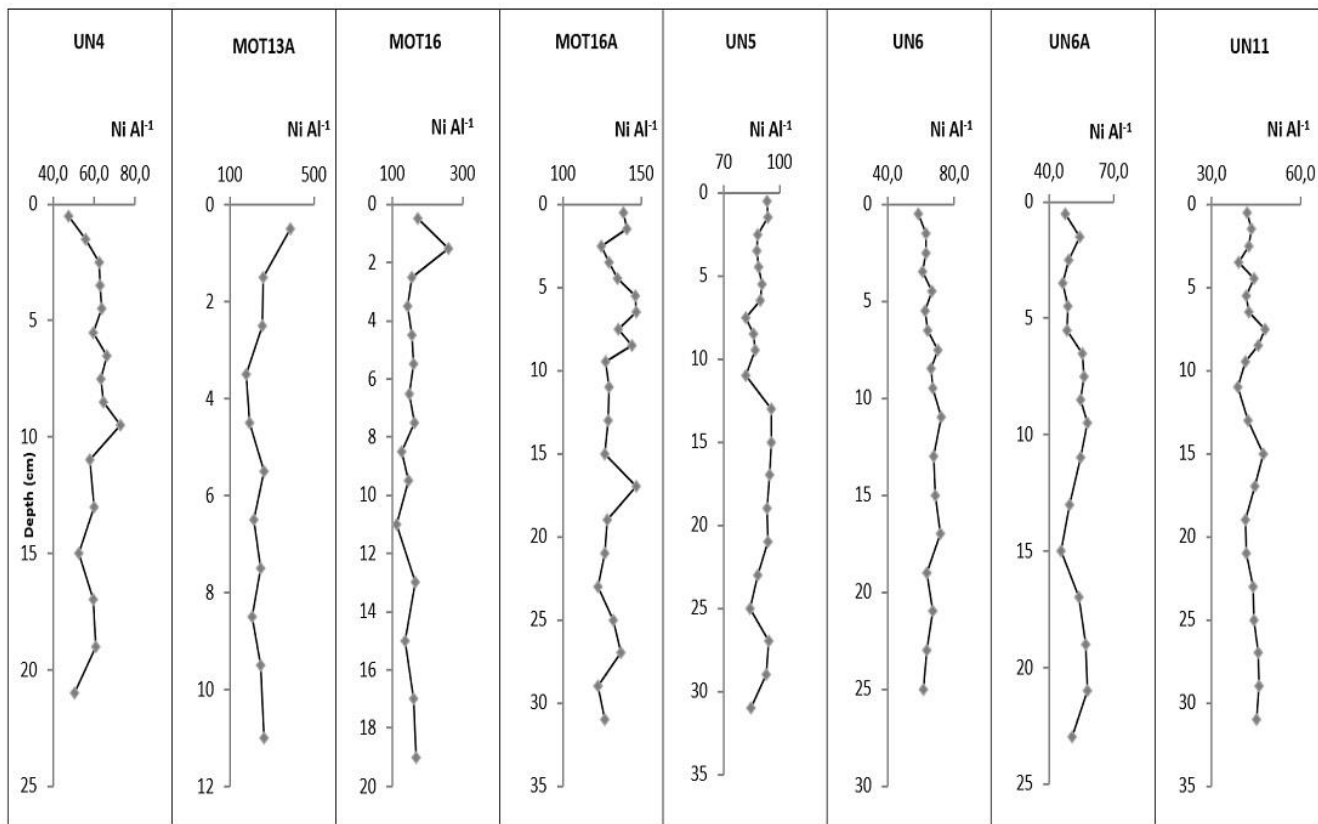
507 calculated at the fine sediment fraction (< 63 µm).



508

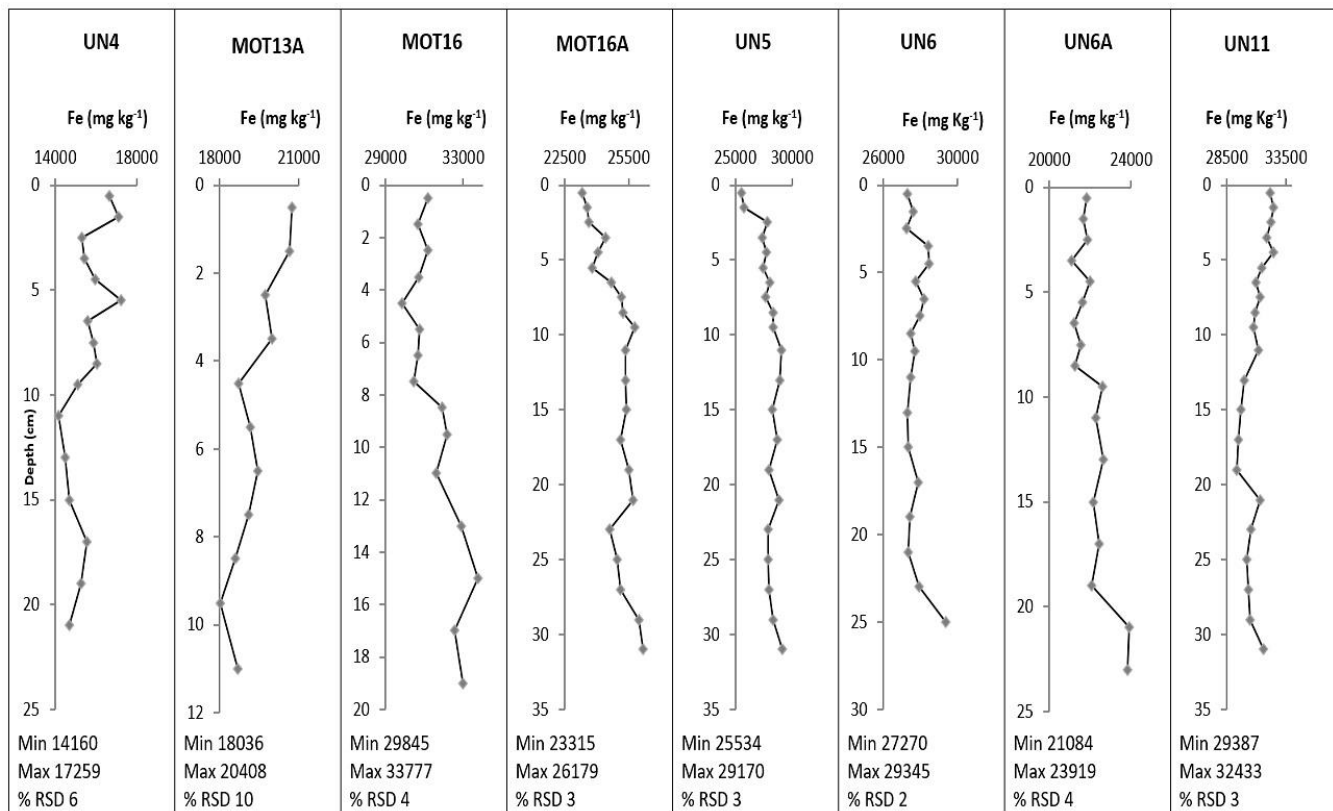
509 **Figure A4: Vertical distributions of Ni in mg kg<sup>-1</sup> in sediment cores. The concentrations in coarse cores MOT13A, MOT16, UN4**

510 refer to the total sediment fraction (< 1 mm).



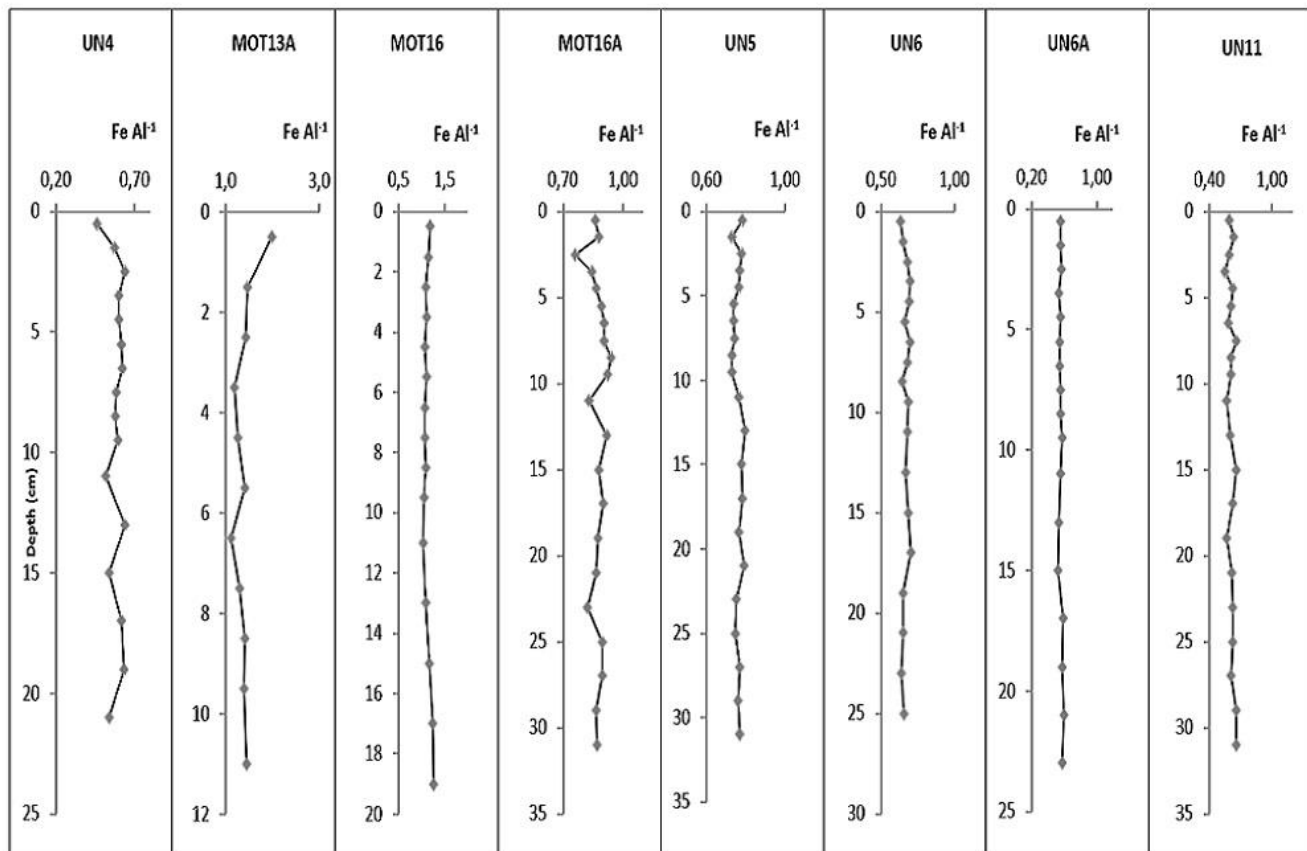
511

512 **Figure A5:** Vertical distributions of  $\text{Ni Al}^{-1} \times (10^4)$  in sediment cores. The ratios in coarse cores MOT13A, MOT16, UN4 are  
 513 calculated at the fine sediment fraction ( $< 63 \mu\text{m}$ ).



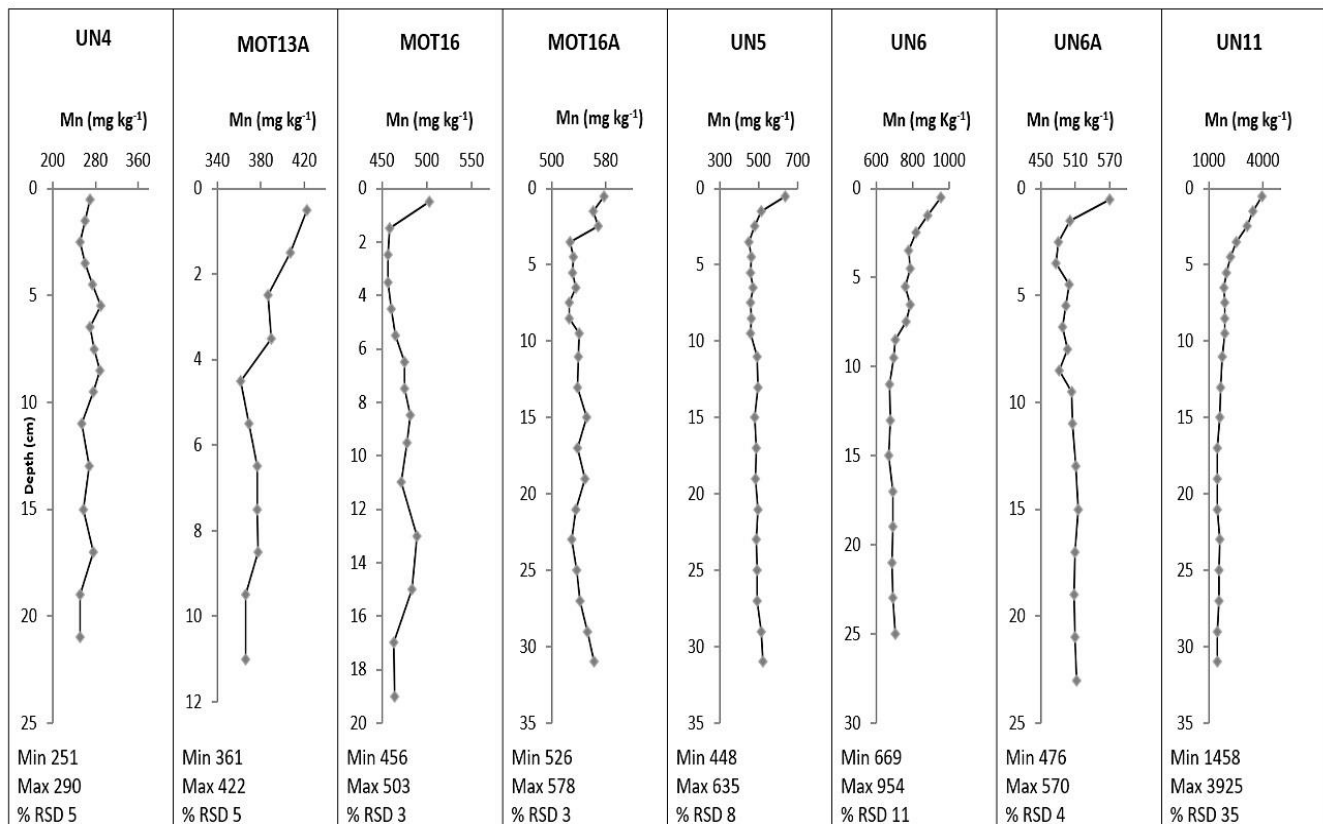
514

515 **Figure A6:** Vertical distributions of  $\text{Fe}$  in  $\text{mg kg}^{-1}$  in sediment cores. The concentrations in coarse cores MOT13A, MOT16, UN4  
 516 refer to the total sediment fraction ( $f < 1 \text{ mm}$ ).



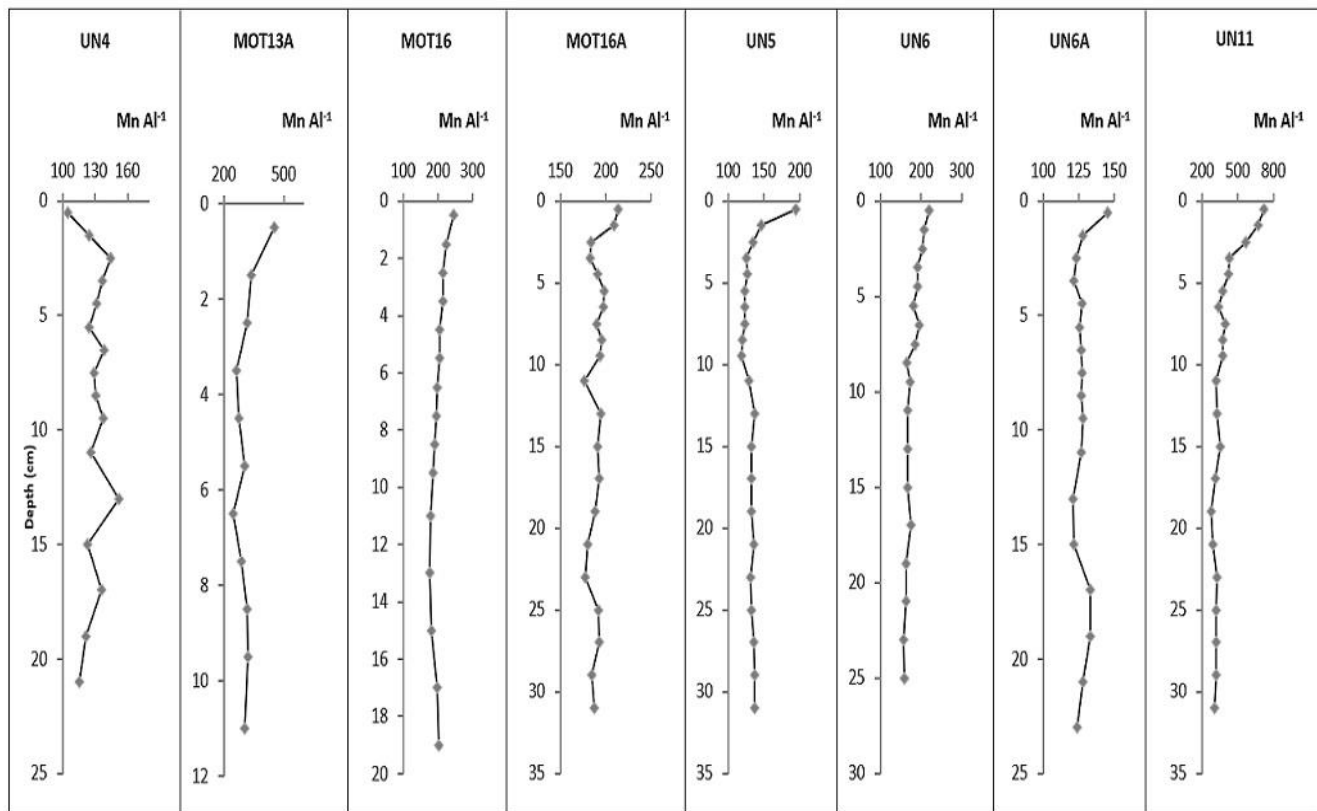
517

518 **Figure A7:** Vertical distributions of  $\text{Fe Al}^{-1}$  in sediment cores. The ratios in coarse cores MOT13A, MOT16, UN4 are calculated at  
519 the fine sediment fraction ( $< 63 \mu\text{m}$ ).



520

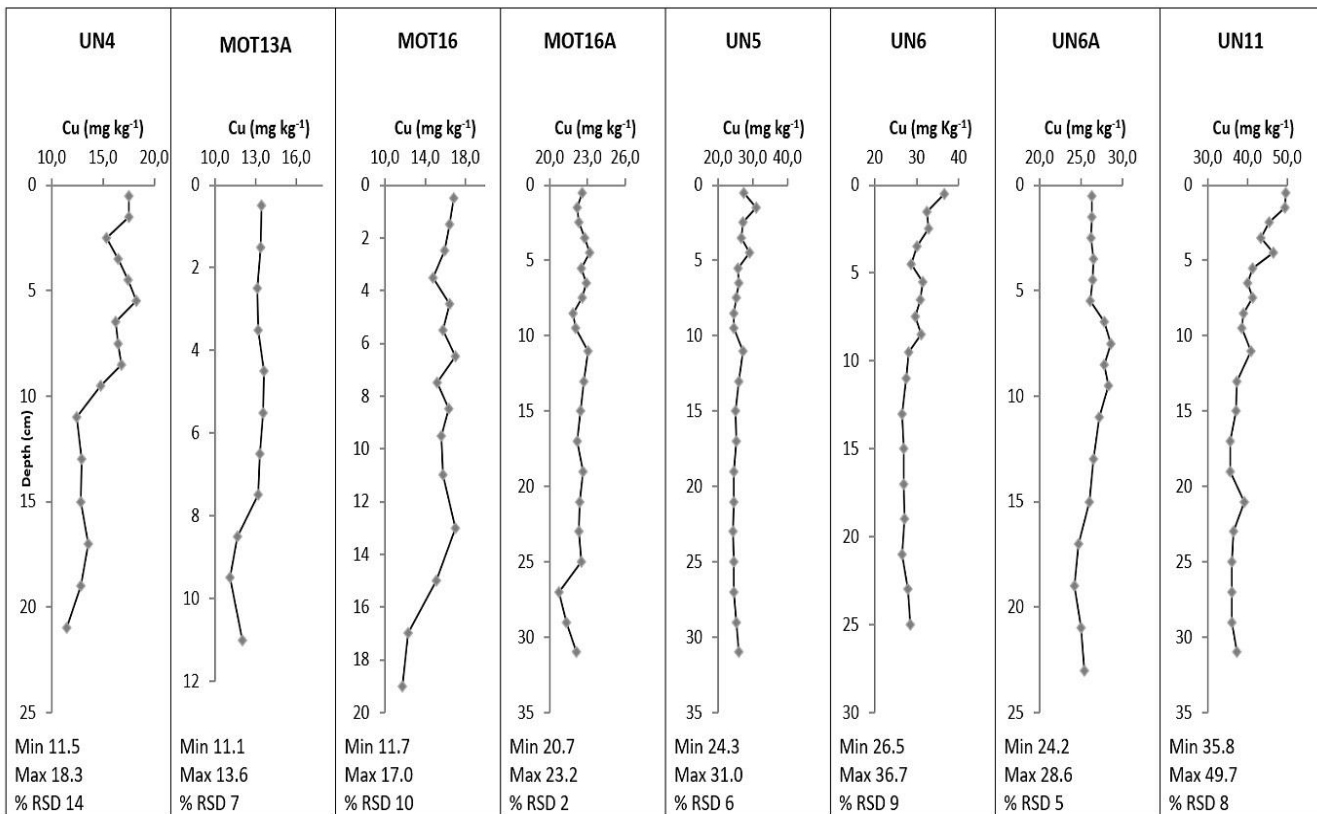
521 **Figure A8:** Vertical distributions of Mn in  $\text{mg kg}^{-1}$  in sediment cores. The concentrations in coarse cores MOT13A, MOT16, UN4  
522 refer to the total sediment fraction ( $< 1 \text{ mm}$ ).



523

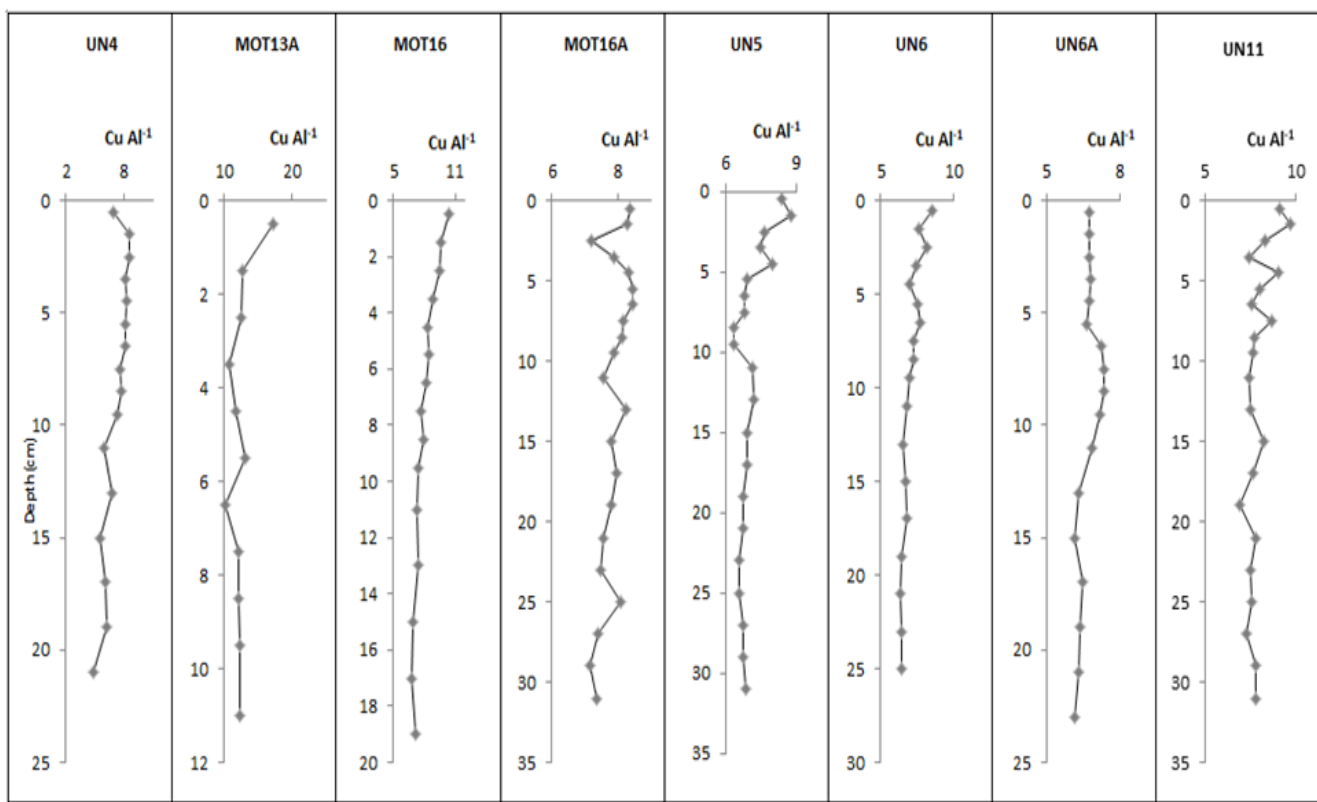
524 **Figure A9:** Vertical distributions of  $\text{Mn Al}^{-1} \times 10^4$  in sediment cores. The ratios in coarse cores MOT13A, MOT16, UN4 are  
 525 calculated at the fine sediment fraction ( $< 63 \mu\text{m}$ ).

526

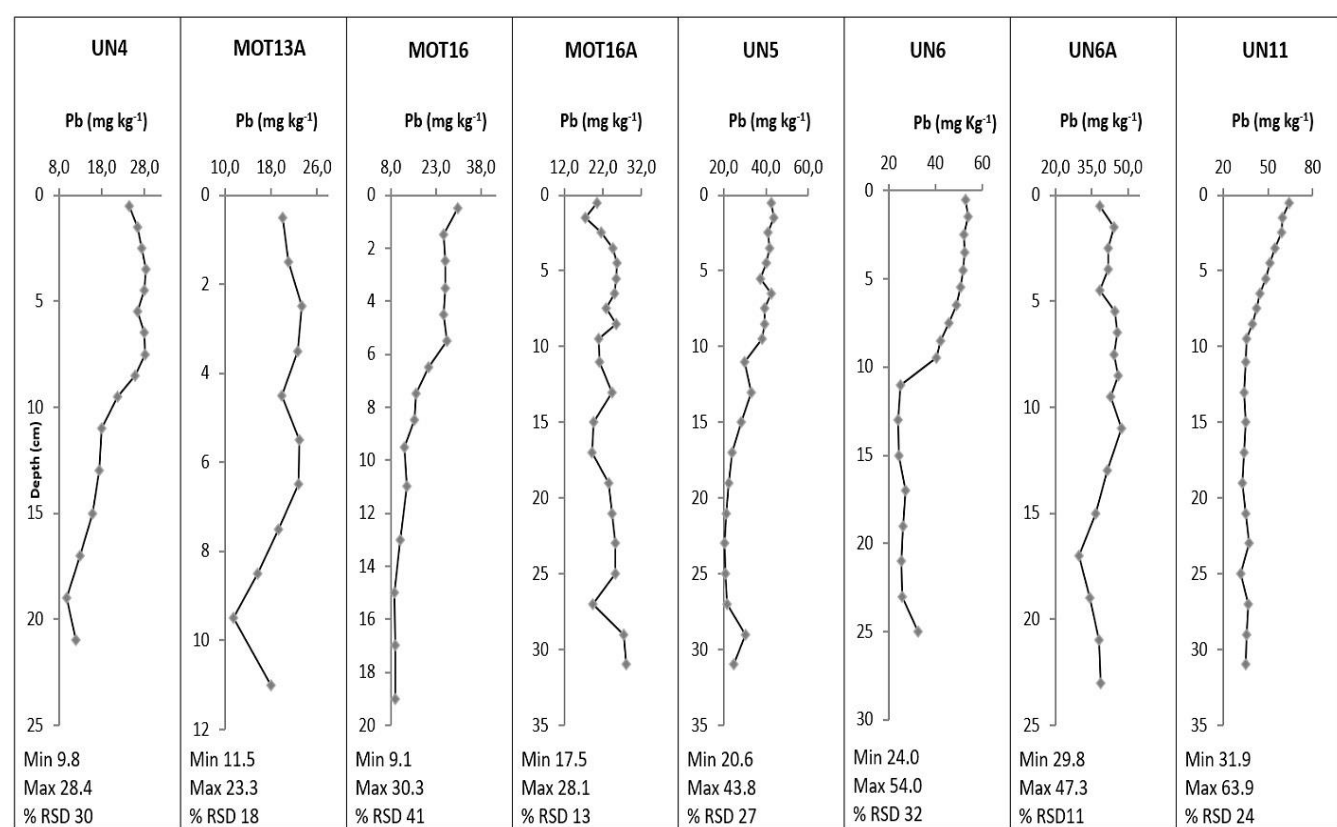


527

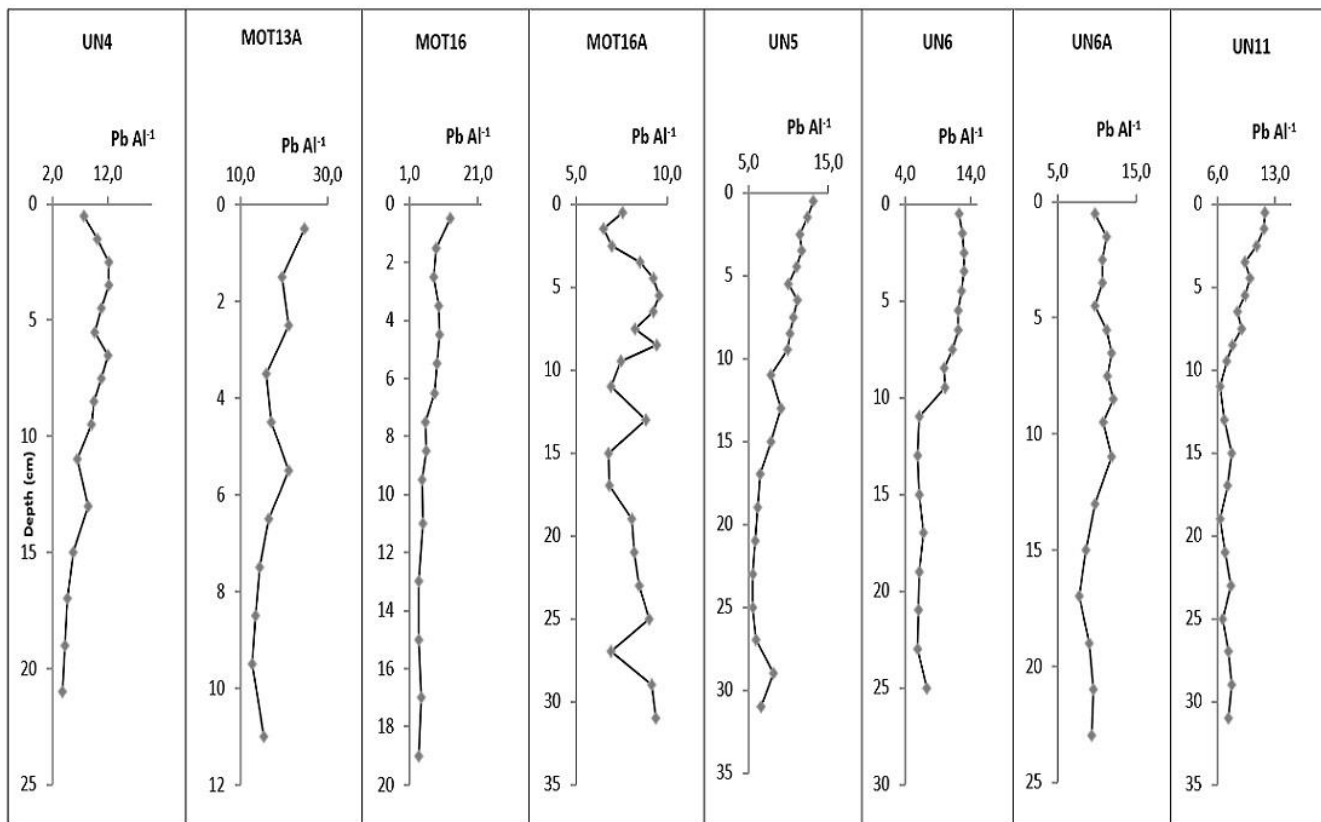
528 **Figure A10:** Vertical distributions of  $\text{Cu}$  in  $\text{mg kg}^{-1}$  in sediment cores. The concentrations in coarse cores MOT13A, MOT16, UN4  
 529 refer to the total sediment fraction ( $< 1 \text{ mm}$ ).



531 **Figure A11:** Vertical distributions of  $\text{Cu Al}^{-1} \times (10^4)$  in sediment cores. The ratios in coarse cores MOT13A, MOT16, UN4 are  
 532 calculated at the fine sediment fraction ( $< 63 \mu\text{m}$ ).  
 533



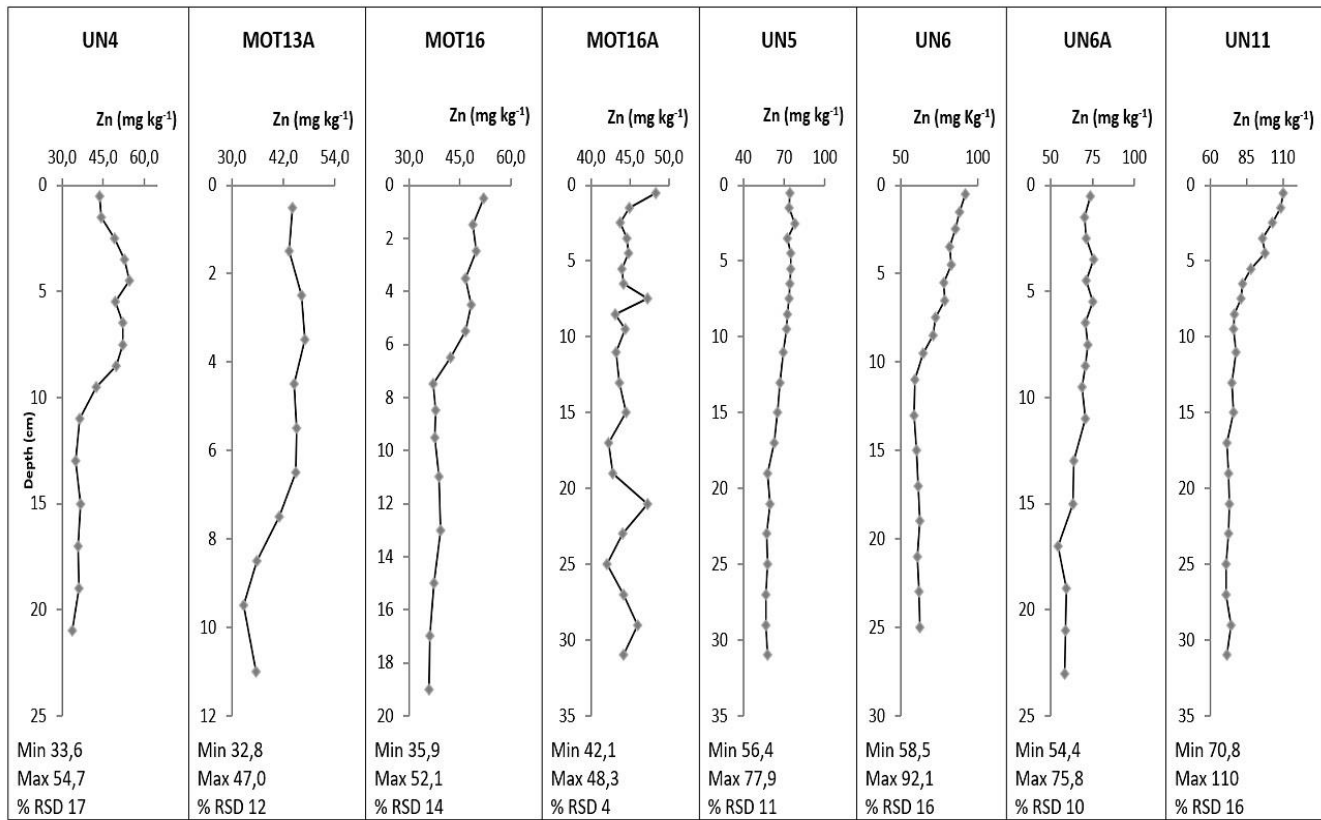
534 **Figure A12:** Vertical distributions of Pb in  $\text{mg kg}^{-1}$  in sediment cores. The concentrations in coarse cores MOT13A, MOT16, UN4  
 535 refer to the total sediment fraction ( $< 1 \text{ mm}$ ).  
 536



537

538  
539

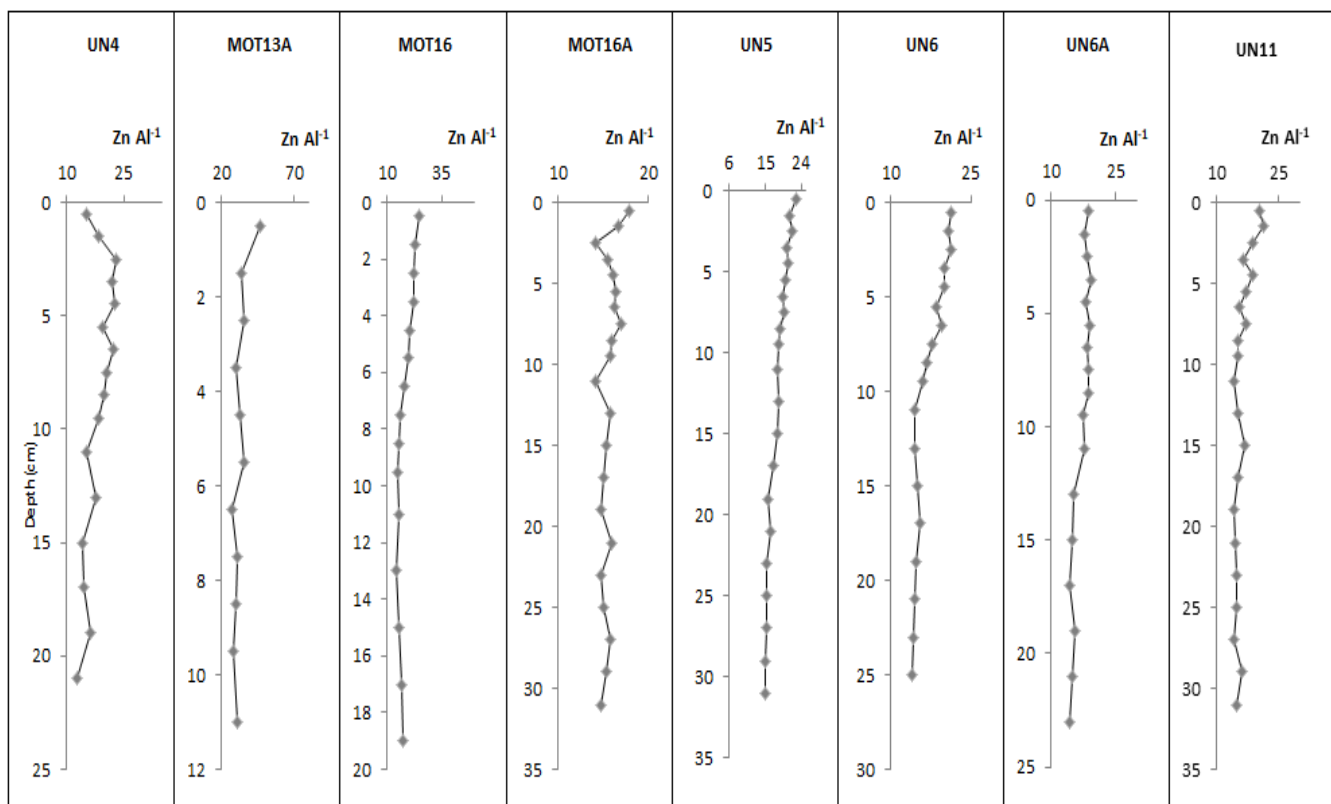
Figure A13: Vertical distributions of  $\text{Pb Al}^{-1} \times (10^4)$  in sediment cores. The ratios in coarse cores MOT13A, MOT16, UN4 are calculated at the fine sediment fraction ( $< 63 \mu\text{m}$ ).



540

541  
542

Figure A14: Vertical distributions of Zn in  $\text{mg kg}^{-1}$  in sediment cores. The concentrations in coarse cores MOT13A, MOT16, UN4 refer to the total sediment fraction ( $< 1 \text{ mm}$ ).



543  
 544 **Figure A15:** Vertical distributions of  $Zn Al^{-1} \times (10^4)$  in sediment cores. The ratios in coarse cores MOT13A, MOT16, UN4 are  
 545 calculated at the fine sediment fraction ( $< 63 \mu m$ ).

546

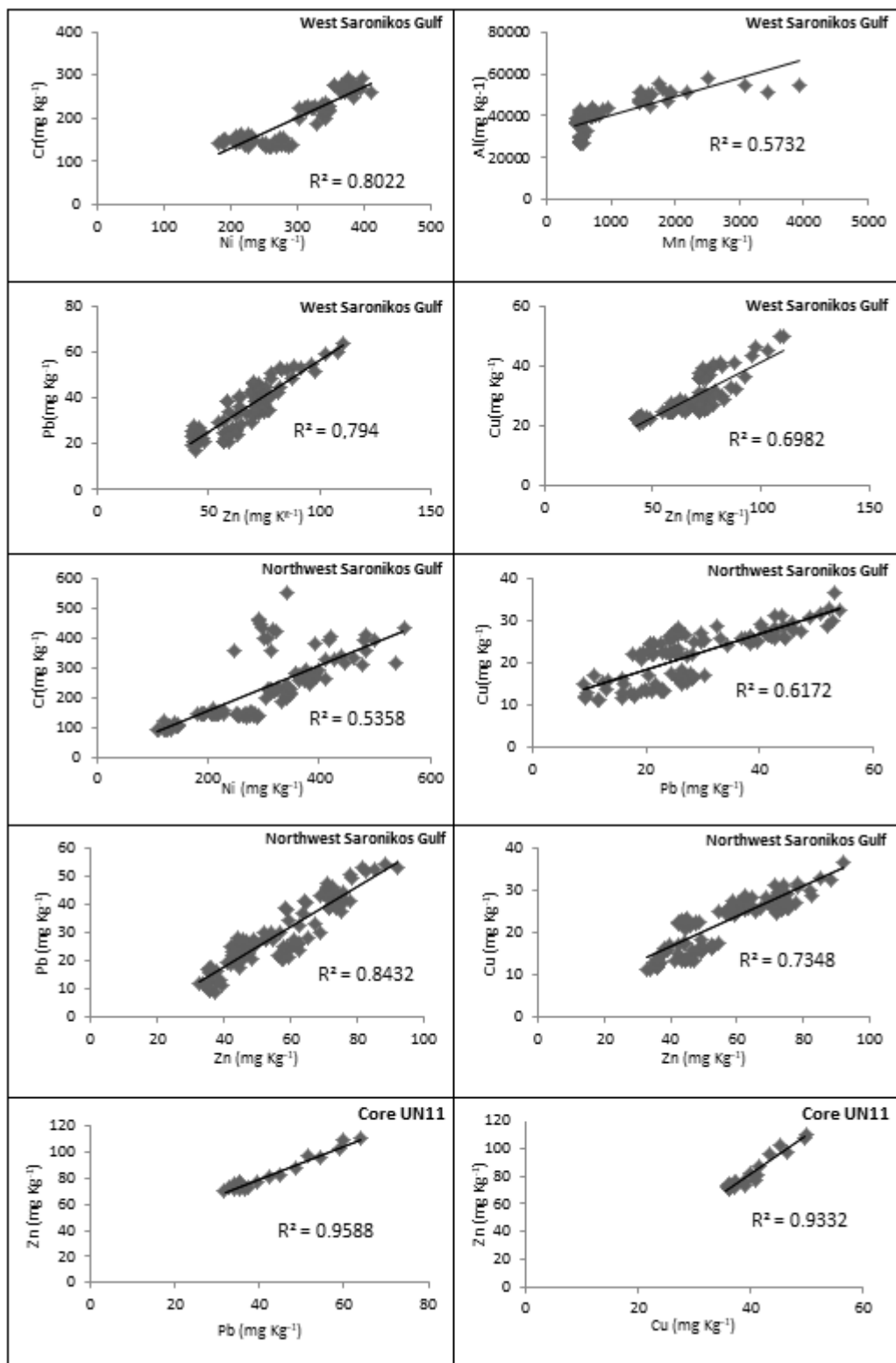
547 **Table A3. Spearman's correlation coefficient matrix for Al (mg Kg⁻¹), Cr (mg Kg⁻¹), Ni (mg Kg⁻¹), Fe (mg Kg⁻¹), Mn (mg Kg⁻¹), Cu**  
 548 **(mg Kg⁻¹), Pb (mg Kg⁻¹), Zn (mg Kg⁻¹), TOC (% Total Organic Carbon), carbonates (% CaCO₃) (N=140 sediment samples).**

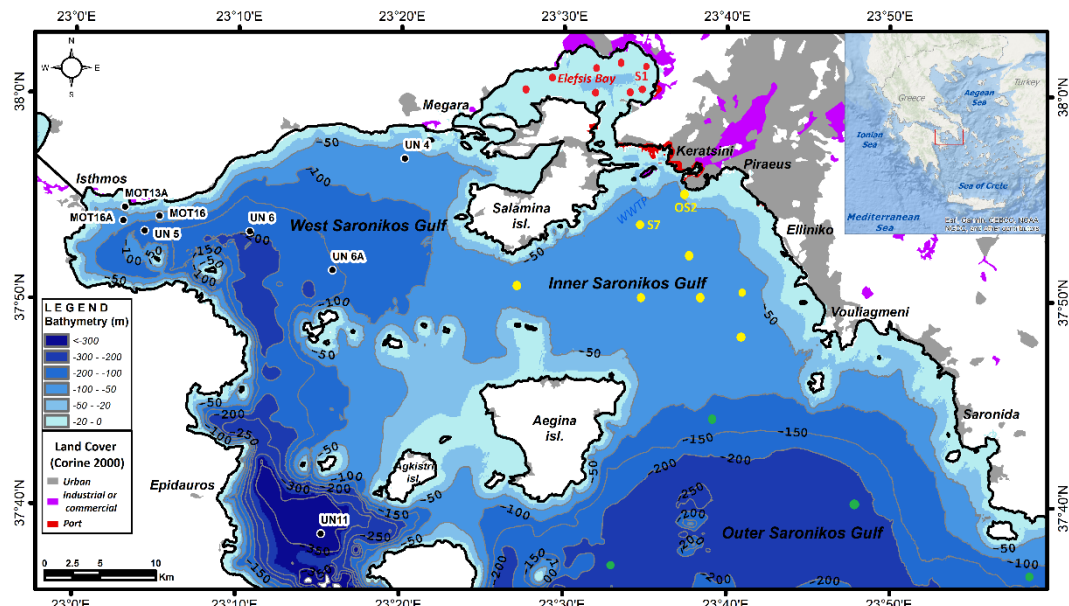
549

| Correlations        |          |          |          |          |          |          |          |          |          |                        |
|---------------------|----------|----------|----------|----------|----------|----------|----------|----------|----------|------------------------|
| Spearman's<br>rho   | Al       | Cr       | Ni       | Fe       | Mn       | Cu       | Pb       | Zn       | TOC      | %<br>CaCO <sub>3</sub> |
| Al                  | 1.000    |          |          |          |          |          |          |          |          |                        |
| Cr                  | -0.521** | 1.000    |          |          |          |          |          |          |          |                        |
| Ni                  | -0.453** | 0.841**  | 1.000    |          |          |          |          |          |          |                        |
| Fe                  | 0.624**  | 0.081    | 0.179*   | 1.000    |          |          |          |          |          |                        |
| Mn                  | 0.735**  | -0.108   | 0.029    | 0.694**  | 1.000    |          |          |          |          |                        |
| Cu                  | 0.924**  | -0.419** | -0.342** | 0.633**  | 0.746**  | 1.000    |          |          |          |                        |
| Pb                  | 0.676**  | -0.440** | -0.433** | 0.244**  | 0.397**  | 0.779**  | 1.000    |          |          |                        |
| Zn                  | 0.790**  | -0.452** | -0.441** | 0.459**  | 0.479**  | 0.882**  | 0.894**  | 1.000    |          |                        |
| TOC                 | 0.244**  | -0.198*  | -0.272** | 0.096    | 0.155    | 0.351**  | 0.428**  | 0.483**  | 1.000    |                        |
| % CaCO <sub>3</sub> | -0.472** | -0.215*  | -0.222** | -0.766** | -0.597** | -0.566** | -0.358** | -0.516** | -0.282** | 1.000                  |

550 \*\*. Correlation is significant at the 0.01 level (2-tailed).

552 \*. Correlation is significant at the 0.05 level (2-tailed).

554  
555  
556  
557  
558  
559  
560  
561  
562  
563  
564  
565  
566  
567  
568  
569  
570  
571  
572  
573  
574  
575  
Figure A16: Correlations of heavy metals for the core samples of West Saronikos Gulf.



578 **Figure A17: Map of Saronikos with stations in Elefsis Bay (red circles), Inner Saronikos (yellow circles) and Outer Saronikos (green circles) from which metal concentrations in sediments were review for the comparative discussion to the present study results in**

579 **West Saronikos (black circles).**

## 582 **8 Data availability**

583 Datasets and their sources are fully detailed in the manuscript.

## 585 **9 Team list**

586 Not applicable.

## 588 **10 Author contribution**

589 Georgia Filippi and Vasiliki Paraskevopoulou conducted the chemical analyses in the Laboratory of Environmental Chemistry  
 590 of the National and Kapodistrian University of Athens. Georgia Filippi wrote the paper, with contributions and reviews from  
 591 all co-authors. Konstantinos Lazogiannis constructed the map of the study area and contributed to compilation and  
 592 improvements of figures. Manos Dassenakis was the supervisor of the laboratory work and this article.

## 594 **11 Competing interests**

595 The authors declare that they have no conflict of interest.

## 597 **12 Special issue statement**

598 The statement on a corresponding special issue will be included by Copernicus, if applicable.

## 600 **13 Acknowledgements**

601 We are grateful to the Hellenic Center for Marine Research (HCMR) and our colleagues Prof. S. Poulos, Dr Aik. Karditsa, and  
 602 Dr F. Botsou for the assistance during the sampling. The research was funded by the European Union (European Social Fund)  
 603 and National Funds (Hellenic General Secretariat for Research and Technology) in the framework of the project ARISTEIA  
 604 I, 640 “Integrated Study of Trace Metals Biogeochemistry in the Coastal Marine Environment”, within the “Lifelong Learning  
 605 Programme”. This project gave us the opportunity to reach the heavy metal pollution of West Saronikos Gulf. This paper  
 606 summarizes the results of this study.

607 **14 References**

608 AOAC INTERNATIONAL: Appendix F: Guidelines for Standard Method Performance Requirements, AOAC Official  
609 Methods of Analysis, [http://www.eoma.aoac.org/app\\_f.pdf](http://www.eoma.aoac.org/app_f.pdf), 2016.

610

611 Barjy, M., Maanan, M., Maanan, M., Salhi, F., Tnoumi, A., and Zourarah, B.: Contamination and environmental risk  
612 assessment of heavy metals in marine sediments from Tahaddart estuary (NW of Morocco), *Hum. Ecol. Risk Assess.*, 26, 71-  
613 86, <https://doi.org/10.1080/10807039.2018.1495056>, 2020.

614

615 Bigus, P., Tobiszewski, M., and Namiesnik, J.: Historical records of organic pollutants in sediment cores, *Mar. Poll. Bull.*, 78,  
616 26-42, <https://doi.org/10.1016/j.marpolbul.2013.11.008>, 2014.

617

618 Chen, X., Li, S., Newby, S.M., Lyons, T.W., Wu, F., Owens, J.D.: Iron and manganese shuttle has no effect on sedimentary  
619 thallium and vanadium isotope signatures in Black Sea sediments, *Geochim. Cosmochim. Ac.*, 317, 218233,  
620 <https://doi.org/10.1016/j.gca.2021.11.010>, 2022

621

622 Dassenakis, M., Scoullos, M., Rapti, K., Pavlidou., A., Tsorova, D., Paraskevopoulou, V., Rozi, E., Stamateli, A., and Siganos,  
623 M.: The distribution of copper in Saronicos Gulf after the operation of the wastewater treatment plant of Psitalia, *Global Nest*  
624 J., 5, 135-145, <https://doi.org/10.30955/gnj.000282>, 2003.

625

626 Diamantopoulou, A., Kalavrouziotis, I.K., and Varnavas, S.P.: Geochemical investigations regarding the variability of metal  
627 pollution in the Amvrakikos Bay *Global Nest J.*, 21, 7-13, <https://doi.org/10.30955/gnj.002733>, 2019.

628

629 Gredilla, A., Stoichev., T., Fdez-Ortiz de Vallejuelo, S., Rodriguez-Iruretagoiena, A., Morais, P., Arana, G., and Madariaga,  
630 J.M.: Spatial distribution of some trace and major elements in sediments of the Cávado estuary (Esposende, Portugal), *Mar.*  
631 *Poll. Bull.*, 99, 305-311, <https://doi.org/10.1016/j.marpolbul.2015.07.040>, 2015.

632

633 Hahladakis, J., Smaragnaki, E., Vasilaki, G., and Gidaragos, E.: Use of Sediment Quality Guidelines and pollution indicators  
634 for the assessment of heavy metal and PAH contamination in Greek surficial sea and lake sediments, *Env. Mon. Assess.*, 185,  
635 2843-2853, <https://doi.org/10.1007/s10661-012-2754-2>, 2012.

636

637 Jackson, M.L.: Soil Chemical Analysis, *Soil Sci. Soc. Am. J.*, 22, 272-272,  
638 <https://doi.org/10.2136/sssaj1958.03615995002200030025x>, 1958.

639

640 Kanellopoulos, T., Kapetanaki, N., Karaouzas, I., Botsou, F., Mentzafou, A., Kaberi, H., Kapsimalis, V., and Karageorgis, A.:  
641 Trace element contamination status of surface marine sediments of Greece: an assessment based on two decades (2001–2021)  
642 of data, *Environ. Sci. Pollut. R.*, 29, 45171-45189, <https://doi.org/10.1007/s11356-022-20224-y>, 2022.

643

644 Karageorgis, A.P., Kaberi, H., Price, N.B., Muir, G.K.P., Pates, J.M., and Lykousis, V.: Chemical composition of short  
645 sediment cores from Thermaikos Gulf (Eastern Mediterranean): Sediment accumulation rates, trawling and winnowing effects,  
646 *Cont. Shelf Res.*, 25, 2456–2475, <https://doi.org/10.1016/j.csr.2005.08.006>, 2005.

647

648 Karageorgis, A.P., Botsou, F., Kaberi, H., and Iliakis, H.: Geochemistry of major and trace elements in surface sediments of  
649 the Saronikos Gulf (Greece): Assessment of contamination between 1999 and 2018, *Sci. Total Environ.*, 717, 137046,  
650 <https://doi.org/10.1016/j.scitotenv.2020.137046>, 2020.

651

652 Karageorgis, A.P., Botsou, F., Kaberi, H., and Iliakis, H.: Dataset on the major and trace elements contents and contamination  
653 in the sediments of Saronikos Gulf and Elefsis Bay, Greece, *Data in brief*, *Sci. Total Environ.*, 29, 2352-3409,  
654 <https://doi.org/10.1016/j.dib.2020.105330>, 2020a.

655

656 Kelepertsis, A., Alexakis, D., and Kita, I.: Environmental Geochemistry of soils and waters of Susaki Area, Korinthos, Greece,  
657 *Environ. Geochem. Hlth*, 23, 117-135, <https://doi.org/10.1023/A:1010904508981>, 2001.

658

659 Kiratli, N., Ergin, M.: Partitioning of heavy metals in surface Black Sea sediments, *Appl. Geochem.*, 11 (6), 775-788,  
660 [https://doi.org/10.1016/S0883-2927\(96\)00037-6](https://doi.org/10.1016/S0883-2927(96)00037-6), 1996

661

662 Kontoyiannis, H.: Observations on the circulation of the Saronikos Gulf: A Mediterranean embayment sea border of Athens,  
663 *J. Geophys. Res.*, 115, <https://doi.org/10.1029/2008JC005026>, 2010.

664

665 Long, E.R., MacDonald, D.D., Smith, S.L., and Calder, F.D.: Incidence of Adverse Biological Effects Within Ranges of  
666 Chemical Concentrations in Marine and Estuarine Sediments, *Environ. Manage.*, 19, 81-97,  
667 <https://doi.org/10.1007/BF02472006>, 1995.

668

669 Loring, H.D., and Rantala, R.: Manual for the Geochemical Analyses of Marine Sediments and Suspended Particulate Matter.  
670 *Earth-Sci. Rev.*, 32, 235-283, [http://dx.doi.org/10.1016/0012-8252\(92\)90001-A](http://dx.doi.org/10.1016/0012-8252(92)90001-A), 1992.

671

672 Manahan, E.: Water Chemistry, Green Science and Technology of Nature's Most Renewable Resource, 1<sup>st</sup> edition, CRC Press,  
673 Taylor & Francis Group, U.S., 416 pp., 2011.

674

675 Nolting, R.F., Ramkema, A., and Everaarts, J.M.: The geochemistry of Cu, Cd, Zn, Ni and Pb in sediment cores from the  
676 continental slope of the Banc d'Arguin (Mauritania), *Cont. Shelf Res.*, 19, 665 -691, [https://doi.org/10.1016/S0278-4343\(98\)00109-5](https://doi.org/10.1016/S0278-4343(98)00109-5), 1999.

677

678

679 Ozturk, M.: Trends of trace metal (Mn, Fe, Co, Ni, Cu, Zn, Cd and Pb) distributions at the oxic-anoxic interface and in sulfidic  
680 water of the Drammensfjord, *Mar. Chem.*, 48, 329-342, [https://doi.org/10.1016/0304-4203\(95\)92785-Q](https://doi.org/10.1016/0304-4203(95)92785-Q), 1995.

681

682 Panagiotoulias, I., Botsou, F., Kaberi, H., Karageorgis, A.P. and Scoullos, M.: Can we document if regulation and Best  
683 Available Techniques (BAT) have any positive impact on the marine environment? A case based on a steel mill in Greece,  
684 *Environ. Monit. Assess.*, 189: 598, <https://doi.org/10.1007/s10661-017-6324-5>, 2017.

685

686 Panagopoulou, G., Heavy metals (Hg, Pb, Cd) at water samples and sediments of Saronikos Gulf, MSc thesis (in Greek),  
687 University of Athens in Greece, Greece, 2018.

688

689 Paraskevopoulou, V.: Distribution and chemical behaviour of heavy metals in sea area affected by industrial pollution (NW  
690 Saronikos), PhD Thesis in Chemical Oceanography (in Greek), University of Athens in Greece, Greece, 2009.

691 Paraskevopoulou, V., Zeri, C., Kaberi, H., Chalkiadaki, O., Krasakopoulou, E., Dassenakis, M., and Scoullos, M.: Trace metal  
692 variability, background levels and pollution status assessment in line with the water framework and Marine Strategy  
693 Framework EU Directives in the waters of a heavily impacted Mediterranean Gulf, Mar. Poll. Bull., 87, 323-337,  
694 <https://doi.org/10.1016/j.marpolbul.2014.07.054>, 2014.

695

696 Pavlidou, A., Kontoyiannis, H., and Psyllidou-Giouranovits, R.: Trophic conditions and stoichiometric nutrient balance in the  
697 Inner Saronic Gulf (Central Aegean Sea) affected by the Psitalia seawage outfall, Fresenius Environ. Bull., 13, 12b.,  
698 [https://www.prt-parlar.de/download\\_feb\\_2004/](https://www.prt-parlar.de/download_feb_2004/), 2004.

699

700

701 Peña-Icart, M., Villanueva, M., Alonso Hernández, C., Rodríguez Hernández, J., Behar, M., and Pomares Alfonso, M.:  
702 Accepted Manuscript, Comparative Study of Digestion Methods EPA 3050B (HNO<sub>3</sub>-H<sub>2</sub>O<sub>2</sub>-HCl) and ISO 11466.3 (aqua regia)  
703 for Cu, Ni and Pb Contamination Assessment in Marine Sediments, Mar. Env. R., 60-66, <https://hal.archives-ouvertes.fr/hal-00720186/document>, 2011.

704

705

706 Pohl, C., and Hennings, U.: The effect of redox processes on the partitioning of Cd, Pb, Cu, and Mn between dissolved and  
707 particulate phases in the Baltic Sea, Mar. Chem., 65, 41-53, [https://doi.org/10.1016/S0304-4203\(99\)00009-2](https://doi.org/10.1016/S0304-4203(99)00009-2), 1999.

708

709 Prifti, E, Kaberi, H., Paraskevopoulou, V., Michalopoulos, P., Zeri, C., Iliakis, S., Dassenakis, M., and Scoullos, M.: Vertical  
710 distribution and chemical fractionation of heavy metals in dated sediment cores from the Saronikos Gulf, Greece, J. Mar. Sci.  
711 Eng., 10, 376, <https://doi.org/10.3390/jmse10030376>, 2022.

712

713 Psyllidou-Giouranovits R. and Pavlidou A.: Chemical characteristics in Catsiki V.A. (ed), Pollution research and Monitoring  
714 program in Saronikos gulf, Technical report, 1998 (in Greek).

715

716 Salomons, W. and Förstner, U.: Metals in the Hydrocycle, 1, Springer Berlin, Heidelberg, Berlin, 352 pp.,  
717 <https://doi.org/10.1007/978-3-642-69325-0>, 1984.

718

719 Scoullos, M.: Lead in coastal sediments: The case of Elefsis gulf, Sci. Total Environ., 49, 199-219,  
720 [https://doi.org/10.1016/0048-9697\(86\)90240-8](https://doi.org/10.1016/0048-9697(86)90240-8), 1986.

721

722 Scoullos, M., Sakellari, A., Giannopoulou, K., Paraskevopoulou, V., and Dassenakis, M.: Dissolved and particulate trace metal  
723 levels in the Saronikos Gulf, Greece, in 2004. The impact of the primary Wastewater Treatment Plant of Psitalia, Desalination,  
724 210, 98-109, <https://doi.org/10.1016/j.desal.2006.05.036>, 2007.

725

726 Skoog, D., Holler, F.J., and Nieman, T. A.: Principles of Instrumental Analysis, Fifth Edition, Saunders golden sunburst series,  
727 Saunders College Pub., Philadelphia , Orlando, Fla., Harcourt Brace College Publishers, 1998.

728

729 SoHelME, Papathanassiou, E. & Zenetos, A. (eds): State of the Hellenic Marine Environment., HCMR Publ., 360 pp,  
730 <https://epublishing.ekt.gr/sites/ektpublishing/files/ebooks/Sohelme.pdf>, 2005.

731

732 Sundby, B.: Transient state diagenesis in continental margin muds, Mar. Chem., 102 (1-2), 2-12,  
733 <https://doi.org/10.1016/j.marchem.2005.09.016>, 2006.

734 Sutherland, R.A.: Bed sediment-associated trace metals in an urban stream, Oahu, Hawaii, Env. Geol., 39, 611-627,  
735 <https://doi.org/10.1007/s002540050473>, 2000.

736

737 US EPA: Method 3050B Acid Digestion of sediments, sludges and soils, 1996, Revision 2,  
738 <https://www.epa.gov/sites/default/files/2015-06/documents/epa-3050b.pdf>, 1996.

739

740 Vrettou, E.: Heavy metals in sediment cores of Saronikos Gulf, MSc thesis (in Greek), University of Athens in Greece, Greece,  
741 2019.

742

743 Walkley, A.: A Critical Examination of a Rapid Method for Determining Organic Carbon in Soils: Effect of Variations in  
744 Digestion Conditions and of Inorganic Soil Constituents. Soil Sc., 63, 251-264,  
745 <http://dx.doi.org/10.1097/00010694-194704000-00001>, 1947.

746

747 Xarlis, P.: Heavy metals (Cu, Ni, Zn) at water samples and sediments of Saronikos Gulf, MSc thesis (in Greek), University of  
748 Athens in Greece, Greece, 2018.